JOURNAL OF PETROLOGY | VOLUME 37 | NUMBER 4 | PAGES 927–959 | 1996

PAUL R. D. MASON[1]*, HILARY DOWNES[1], MATTHEW F. THIRLWALL[2], IOAN SEGHEDI[3], ALEXANDRU SZAKÁCS[3], DAVID LOWRY[2] AND DAVID MATTEY[2]

[1]RESEARCH SCHOOL OF GEOLOGICAL AND GEOPHYSICAL SCIENCES, BIRKBECK AND UNIVERSITY COLLEGES, GOWER STREET, LONDON WC1E 6BE, UK

[2]DEPARTMENT OF GEOLOGY, ROYAL HOLLOWAY UNIVERSITY OF LONDON, EGHAM HILL, EGHAM, SURREY TW20 0EX, UK

[3]GEOLOGICAL INSTITUTE OF ROMANIA, STR. CARANSEBES 1, 78344 BUCHAREST 32, ROMANIA

Crustal Assimilation as a Major Petrogenetic Process in the East Carpathian Neogene and Quaternary Continental Margin Arc, Romania

Miocene to Pleistocene calc-alkaline volcanism in the East Carpathian arc of Romania was related to the subduction of a small ocean basin beneath the continental Tisza–Dacia microplate. Volcanic products are predominantly andesitic to dacitic in composition, with rare basalts and rhyodacites (51–71% SiO_2; mg-number 0·65–0·26) and have medium- to high-K calc-alkaline and shoshonitic affinities. Mg, Cr and Ni are low in all rock-types, indicating the absence of primary erupted compositions. Detailed trace element and Sr, Nd, Pb and O isotope data suggest that magmas were strongly crustally contaminated. Assimilation and fractional crystallization (AFC) calculations predict the consumption of 5–35% local upper-crustal metasediments or sediments from the palaeo-accretionary wedge. Variations in the isotopic composition of the contaminants and parental magmas caused variations in the mixing trajectories in different parts of the arc. The most primitive isotopic compositions are found in low-K dacites of the northern Călimani volcanic centre and are interpreted as largely mantle derived. A second possible mantle reservoir of lower $^{143}Nd/^{144}Nd$ and lower $^{206}Pb/^{204}Pb$ is identified from back-arc basic calc-alkaline rocks in the south of the arc. Both magmatic reservoirs have elevated isotopic characteristics, owing either to source bulk mixing (between depleted or enriched asthenosphere and <1% average subducted local sediment) or lower-crustal contamination.

KEY WORDS: *Carpathians; assimilation; calc-alkaline; Sr–Nd–Pb–O isotopes; laser fluorination*

INTRODUCTION

Controls on magmatism in continental margin arc environments are extremely complex, with most arcs showing evidence for significant contamination by continental material either through mantle source enrichment (e.g. Thirlwall, 1982; Ellam *et al.*, 1988; Stern, 1991) or crustal assimilation (e.g. James, 1982; Leeman, 1982; Davidson *et al.*, 1990). Variations in crustal thickness (Hildreth & Moorbath, 1988) and the type of contaminant involved in assimilation (Wörner *et al.*, 1992) have been cited as controls on radiogenic isotope systematics of continental arc magmas. Combined trace element and Sr–Nd–Pb isotope studies have been used to attempt to quantify the mechanism of crustal assimilation (e.g. DePaolo, 1981; Aitcheson & Forrest, 1994).

Neogene to Quaternary volcanic activity of the Eastern Carpathians (Romania) forms the youngest and most south-easterly segment of the subduction-related Inner Carpathian continental margin arc. Here we report the first detailed geochemical and isotopic study for calc-alkaline magmas from the East Carpathian arc and present evidence that crustal contamination was a significant process during magma genesis. We attempt to identify the crustal lithologies involved in assimilation and show how their variation affects the composition of the erupted magmas. Mantle source enrichment and lower-crustal assimilation are discussed as processes

*Present address: NERC ICP-MS Facility, Centre for Analytical Research in the Environment, Imperial College, Silwood Park, Ascot, Berkshire SL5 7TE, UK. Telephone: 01344 294514. Fax: 01344 873997. e-mail: p.r.mason@ic.ac.uk

which may have led to slightly enriched isotopic signatures in the most parental magmas.

Tertiary–Quaternary magmatism in the Carpatho-Pannonian area

Magmatism in the Carpatho-Pannonian region occurred in response to contemporaneous collision and extension (Szabó *et al.*, 1992). Although subduction was related to Alpine tectonic activity which was initiated during the Cretaceous, a major convergence event occurred in the Miocene (Balla, 1987; Săndulescu, 1988) with extensive subduction around the arcuate Carpathian rim (Rădulescu & Săndulescu, 1973; Csontos *et al.*, 1992). The Inner Carpathian calc-alkaline arc was active from the Neogene to the Quaternary, with predominantly Miocene volcanism in the Western Carpathians of Slovakia and Hungary, and Miocene to Quaternary activity in the East Carpathians in Romania (Szabó *et al.*, 1992). The focus of volcanism shifted along the arc, in a very general sense, from west to east through time (Pécskay *et al.*, 1995*b*). An earlier isotopic study of the Carpathian volcanic arc was concerned with early Miocene calc-alkaline lavas from the Western Carpathians (Salters *et al.*, 1988). Sr, Nd and Pb isotopic signatures for these rocks suggested significant contamination by continental crust during magma genesis. Upper-crustal metasediments were recently proposed as the enriched end-member (Downes *et al.*, 1995*a*). Previous workers have indicated geochemical and Sr isotopic variation within volcanics of the East Carpathians (e.g. Peccerillo & Taylor, 1976; Peltz *et al.*, 1987; Seghedi *et al.*, 1995), much of which was attributed to fractional crystallization and partial melting processes rather than to crustal assimilation.

Behind the Carpathian arc lie the Pannonian and Transylvanian Basins, which underwent extension from late Miocene to Quaternary times. Plio-Pleistocene alkali basalt lavas erupted sporadically in these regions are considered to represent an asthenospheric mantle source enriched by the subduction of sediment along the Carpathian arc (Embey-Isztin *et al.*, 1993; Downes *et al.*, 1995*b*). Petrogenetic modelling of both the calc-alkaline and alkaline magmas in the West Carpathians suggested three-component mixing involving the subducted slab, pristine mantle and continental crust (Salters *et al.*, 1988).

Tectonic evolution and geological background of the East Carpathians

Collision took place between North Eastern Europe and the Intra-Carpathian area during the Cenozoic (Royden & Báldi, 1988; Royden & Burchfiel, 1989). Oceanic crust attached to the European plate (Rădulescu & Săndulescu, 1973) was subducted beneath the Alcapa and Tisza–Dacia microplates to accommodate complex relative plate motions between the European and African continents (Royden, 1988). The subducted crust probably originated from a small basin, analogous to the present-day Black Sea, attached in the north-east to the Scythian–Russian continental platform (Burchfiel, 1976). The main convergence event took place during the Miocene (Balla, 1987; Csontos *et al.*, 1992) during which all of the ocean basin was consumed. Continent–continent collision occurred between the Tisza–Dacia and Scythian blocks at the end of the Miocene. Convergence subsequently waned in magnitude until the present day and tectonic activity is now localized in the extreme south-east of the arc (Horváth, 1988), where deep focus earthquakes still occur at the south-eastern extremity of the East Carpathians (Vrancea zone) (Oncescu *et al.*, 1984).

Calc-alkaline volcanic activity in the Călimani–Gurghiu–Harghita arc (CGHA) took place from late Miocene ($\sim$12 Ma) to Quaternary times ($<$0·2 Ma) (Bleahu *et al.*, 1973; Boccaletti *et al.*, 1973; Peltz *et al.*, 1985; Szabó *et al.*, 1992; Szakács *et al.*, 1993; Pécskay *et al.*, 1995*a*). From north to south, the CGHA consists of the Călimani, Gurghiu and Harghita Mountains (Fig. 1). Călimani is the largest and oldest volcanic centre (11·9–6·7 Ma) (Pécskay *et al.*, 1995*a*). Further south, activity in the six stratovolcanic centres of the Gurghiu Mountains overlapped the later activity of Călimani, but continued later into the Pliocene (9·2–5·4 Ma) (Fig. 1, Table 1). Younger eruptions in the Harghita Mountains overlapped the later stages of Gurghiu volcanism and continued until the Pleistocene. The Harghita Mountains can be divided into a northern (6·3–4·1 Ma) and a southern (2·8–0·2 Ma) section, both consisting of five volcanic centres (Peltz *et al.*, 1973; Seghedi *et al.*, 1986, 1987; Szakács *et al.*, 1993). The most recent magmatism ($<$1 Ma; Szakács *et al.*, 1993) took place in the Southern Harghita Mountains at the extreme south-eastern end of the Inner Carpathians.

To the east of the CGHA (Fig. 1) is a zone of strongly thrust turbidite sediments of Cretaceous to Recent age (Roure *et al.*, 1993), which make up the Outer Carpathians. These represent the uplifted palaeo-accretionary wedge of the Carpathian subduction zone. Flysch and molasse sediments are 6–7 km thick, suggesting that only a small proportion of the sediment overlying the downgoing plate was subducted. Total shortening, estimated from cross-

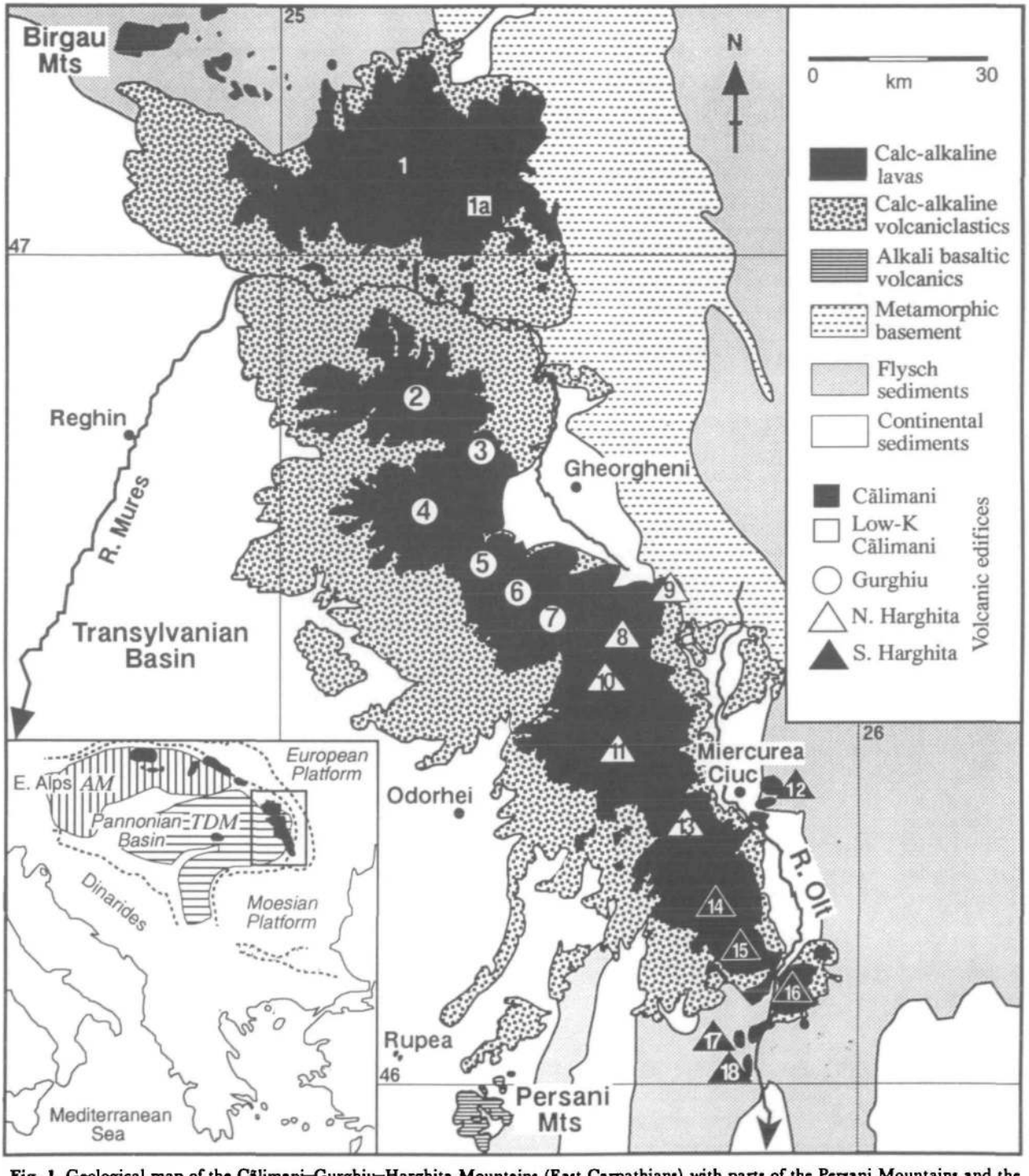

Fig. 1. Geological map of the Călimani–Gurghiu–Harghita Mountains (East Carpathians) with parts of the Persani Mountains and the Birgau Mountains. Key to volcanic edifices: 1, Călimani; 2, Fîncel Lăpusna; 3, Bacta; 4, Seaca Tatarca; 5, Borzont; 6, Sumuleu; 7, Ciumani Fieraestrae; 8, Ostoros; 9, Răchitis; 10, Ivo Cocoizas; 11, Harghita Vîrghis; 12, Sumuleu Ciuc; 13, Luci-Lazu; 14, Cucu; 15, Pilisca; 16, Ciomadul; 17, Murgul Mic; 18, Malnas. The location of the Low-K Călimani group rocks is also shown (a). Modified from the 1:100 000 geological map of Romania (1966, 1990). Inset shows location of the study area with respect to the Eastern Mediterranean and calc-alkaline rocks of the Carpathian arc (filled black regions). Dotted lines are Neogene plate boundaries. AM, Alcapa Microplate; TDM, Tisza–Dacia Microplate.

Table 1: CGHA groups, based on location, age, and geochemical and isotopic characteristics

CGHA group	Constituent volcanic centres	Labels in Fig. 1	Approx. age (Ma)
Low-K Călimani	Outcrops in the Voevodeasa and Lomas valleys, southern part of Călimani	1a	8·6–8·0
Călimani	Călimani (excluding above)	1	9·5–6·5
Gurghiu	Fincel-Lăpusna, Seaca-Tatarca, Bacta, Sumuleu, Ciumani-Fieraestrae	2–7	7·5–5·5
Northern Harghita	Ostoros, Răchitis, Ivo-Cocoizas, Virghis, Luci-Lazu	8–11 and 13	6·0–3·8
Southern Harghita	Cucu, Pilisca, Ciomadul, Malnas, Murgul Mic, Sumuleu-Ciuc (~6 Ma)	12 and 14–18	2·8–0·6

K–Ar age data (Pécskay *et al.*, 1995*a*) shows the approximate age ranges within each group. Luci-Lazu is geographically in the Southern Harghita Mts but has been included in the Northern Harghita group because of its similar chemical and isotopic composition. Similarly, Sumuleu-Ciuc of the Northern Harghita Mts has been included in the Southern Harghita group.

section balancing (Roure *et al.*, 1993), is 130 km for post-Oligocene convergence. In the extreme south of the CGHA and to the north of the Călimani centre, the lavas have been erupted through these sediments.

Continental metamorphic basement of the Tisza–Dacia microplate outcrops immediately to the east of the volcanic arc (Fig. 1). This crustal basement was tectonically active during the Variscan and Alpine orogenies (Pana & Erdmer, 1994) and consists of heterogeneous Precambrian to Cambrian metamorphic rocks of low, intermediate and high grades, together with Mesozoic sedimentary cover (Burchfiel, 1976). Three major lithostratigraphic units have been identified (Burchfiel, 1976; Balintoni & Gheuca, 1977). The lowest unit, the Bretila series, which occurs as discontinuous tectonic wedges, includes micaceous gneisses–paragneisses, metagranitoids and rocks rich in K-feldspar with some amphibolites. Rebra series rocks form the middle unit and consist of paragneiss, amphibolite, mica schist, quartzite and calc-silicates at intermediate depths. The highest tectonic units, the Negrisoara series, include quartzitic paragneiss, schists and gneisses. CGHA magmas have been erupted through all three crustal lithostratigraphic units and may have assimilated this material during ascent.

The Transylvanian Basin borders the East Carpathians to the west and is filled with Neogene to Recent sediments. Mafic alkaline magmas were erupted during the late Pliocene (Downes *et al.*, 1995*b*) at the eastern edge of the basin, ~30 km from the southern end of the CGHA (Fig. 1). These alkali basalts and trachybasalts show subduction-modified trace element signatures with slightly elevated LILE/HFSE (large ion lithophile element to high field strength element) ratios. They contain ultramafic xenoliths, derived from the shallow lithospheric upper mantle (Vaselli *et al.*, 1995), which indicate the presence of depleted mantle beneath the Eastern Transylvanian Basin (the part of the lower lithosphere immediately overlying the mantle wedge of the CGHA).

Two isolated occurrences of calc-alkaline magmatism are situated in the back-arc area, near the outcrops of alkaline volcanics. One is a small plug or lava flow of basaltic andesite at Rupea, ~40 km from the CGHA axis, which has a K/Ar age of 6·81 Ma (Downes *et al.*, 1995*b*) and was therefore contemporaneous with activity in the Gurghiu Mountains. The second is a 2·14-Ma-old lithic block of high-K calc-alkaline basalt from La Gruiu Fintina, which was brought to the surface during a pyroclastic eruption associated with the alkaline magmatism in the Eastern Transylvanian Basin (Downes *et al.*, 1995*b*). This may have been related to volcanism in the Southern Harghita Mountains, although the age, which was determined by K/Ar dating, may have been reset during the pyroclastic eruption.

SAMPLING METHODS AND ANALYTICAL TECHNIQUES

Over 160 samples of volcanic rocks were collected to investigate all major lithologies in the 18 volcanic centres within the CGHA. Samples cover the range in age, geographical and chemical variation noted by previous workers. In addition to *in situ* flows and intrusions, some samples were collected from large blocks in volcaniclastic deposits. A selection of crustal rocks have also been analysed to constrain possible high-level contaminants. Samples of flysch

sediments from the palaeo-accretionary wedge were analysed to constrain the types of sedimentary material which may have been subducted.

Major and trace element abundances were determined on a Philips PW1480 X-ray fluorescence (XRF) spectrometer at the University of London XRF facility at Royal Holloway. Major element oxides were determined on fused glass discs and trace elements on pressed powder pellets with matrix corrections calculated from major element compositions. Selected major and trace element data are included in Table 2. Analytical reproducibility for most trace elements is either about ±1 p.p.m. (2 SD) or ±1%, whichever is greater, but is about ±0·3 p.p.m. for Nb, Rb and Y.

Sr, Nd and Pb isotope analyses (Table 3) were made using standard ion exchange separation techniques and a VG 354 multicollector thermal ionization mass spectrometer at the University of London Radiogenic Isotope Facility at Royal Holloway. Procedures for Sr and Nd isotopes have been described by Thirlwall (1991). A laboratory Nd reference standard (Aldrich) during the period of data acquisition yielded $^{143}Nd/^{144}Nd = 0{\cdot}511425 \pm 9$ (2 SD on 62 analyses), equivalent to a La Jolla value of 0·511857, and SRM987 yielded $^{87}Sr/^{86}Sr = 0{\cdot}710241 \pm 30$ (2 SD on 242 analyses). Samples for Sr isotopic analysis were leached in hot 6 M HCl for 1 h before digestion, to remove the effects of post-magmatic groundmass alteration. However, repeat analyses of leached and unleached samples revealed a minimal difference, within analytical error (e.g. C1-Leached = 0·706850 ± 9, C1-Unleached = 0·706848 ± 11). $^{87}Sr/^{86}Sr$ was normalized to $^{86}Sr/^{88}Sr = 0{\cdot}1194$ to account for mass fractionation. $^{143}Nd/^{144}Nd$ was reproducible to better than 0·000010 and results were normalized for fractionation to $^{146}Nd/^{144}Nd = 0{\cdot}7219$. Leaching for Pb analyses was carried out on 250 μm sieved rock chips in hot 6 M HCl for 1 h. Repeat analyses for both leached and unleached samples gave reproducibility similar to that of standard SRM981. Pb isotopic analyses were normalized for mass fractionation using SRM981, which yielded $^{206}Pb/^{204}Pb = 16{\cdot}891 \pm 12$, $^{207}Pb/^{204}Pb = 15{\cdot}433 \pm 12$, $^{208}Pb/^{204}Pb = 36{\cdot}516 \pm 38$ (2 SD on 54 analyses).

Mineral separates were analysed for O isotope ratios because whole-rock $\delta^{18}O$ ($\delta^{18}O_{WR}$) values can often be affected by late-stage alteration (e.g. Downes *et al.*, 1995*a*). Minerals were separated from a 250 μm fraction using a magnetic separator and by hand picking. Approximately 1 mg of sample was required for each analysis and duplicate analyses were made on all samples. O isotope analyses were carried out at the University of London Stable Isotope Facility at Royal Holloway using a laser fluorination system attached to a VG Isotech PRISM gas-source mass spectrometer fitted with a micro-inlet (Mattey & Macpherson, 1993). Samples were heated with a defocused Nd:YAG laser operating at 1064 nm and fluorinated with ClF_3 at a pressure of 200 mbar. Liberated O_2 was cleaned with KBr and then converted to CO_2 over hot graphite. Sample gases were measured against a laboratory reference gas. Results (Table 3), recorded as $\delta^{18}O$, are given with reference to Vienna Standard Mean Ocean Water (V-SMOW) and are reported as the mean of two or more replicate analyses with external precision typically ±0·1‰ (2 SD). Blank levels were ~0·02 μmol O_2. The technique is sensitive to O_2 yield, which was continuously monitored. Analyses with <95% O_2 yield were discarded. Data from each batch of samples were normalized to a secondary standard (San Carlos olivine) to account for instrumental drift, with typical corrections less than ±0·2‰. Crustal lithologies were not measured by the laser fluorination technique but two samples were analysed by conventional whole-rock Ni-bomb methods at the NERC Isotope Geosciences Laboratory, Keyworth (P. B. Greenwood, personal communication, 1995).

PETROGRAPHY

CGHA lavas vary from basalts, through basaltic andesites, andesites and dacites, to rare rhyodacites. Major phenocryst phases are listed in Table 2. The lavas are typically porphyritic with variable phenocryst assemblages related to the SiO_2 content of the magmas. Plagioclase, magnetite and ilmenite are ubiquitous. Clino- and orthopyroxene are common in basalts, andesites and some dacites. Olivine is recorded in some basalts and basaltic andesites, and amphibole is mainly present in rocks with ≥59% SiO_2. Quartz occurs in rhyodacites, some dacites and in high-K to shoshonitic magmas from the extreme southern end of the arc. Accessory phases include apatite and rare zircon. Sphene is a rare phenocryst phase in some rocks, particularly those from the youngest volcanic centre in the south of the chain. Biotite occurs in the more evolved and more K-rich rocks in the south of the CGHA. A few aphyric rocks, containing only rare plagioclase phenocrysts, occur in several volcanic centres, but most lavas are vitrophyric or fine-grained porphyritic. Two shoshonitic lava domes contain disequilibrium mineralogies with phenocrysts of magnesian olivine, clinopyroxene, plagioclase, quartz, amphibole, biotite and sphene (Mason, 1995; Mason *et al.*, 1995).

Table 2: Major and trace element data for CGHA volcanic and crustal rocks determined by XRF analysis

	Low-K Cãlimani				Cãlimani										
Sample:	C7	C8	C2	C3	C65	C47	C4	C24	C1	C6	C18	C10	C26	C21	C5
SiO_2	62·35	64·11	66·36	68·60	50·73	51·01	51·23	51·58	52·22	53·94	55·83	58·03	59·43	60·74	61·76
Al_2O_3	17·81	17·99	17·61	17·07	19·39	18·06	18·70	18·87	16·47	16·85	18·59	17·51	18·04	18·58	16·56
Fe_2O_3	5·20	4·78	4·32	3·11	9·49	9·82	9·38	9·62	9·53	9·46	8·35	8·09	6·59	6·40	5·55
MgO	1·89	1·12	0·82	0·71	5·14	5·73	4·78	4·90	6·14	4·42	3·85	2·57	3·32	1·67	3·08
CaO	6·55	6·08	5·26	4·20	9·81	9·89	9·84	9·52	8·16	8·35	7·69	6·91	7·05	6·52	4·95
Na_2O	3·80	3·95	4·03	4·43	3·12	2·72	3·26	2·79	3·28	3·10	3·11	3·37	3·25	3·33	3·48
K_2O	1·209	0·918	1·001	1·286	0·871	1·338	0·817	1·410	2·04	1·887	0·990	1·805	1·610	1·910	3·14
TiO_2	0·556	0·528	0·460	0·274	1·084	1·099	1·160	1·095	1·331	0·993	0·890	0·869	0·746	0·635	0·724
MnO	0·168	0·125	0·044	0·118	0·171	0·179	0·231	0·173	0·167	0·176	0·178	0·173	0·138	0·169	0·095
P_2O_5	0·176	0·138	0·130	0·153	0·181	0·247	0·135	0·266	0·362	0·326	0·165	0·193	0·181	0·181	0·223
Total	99·70	99·73	99·94	99·95	100·00	100·09	99·53	100·22	99·71	99·50	99·64	99·52	100·36	100·13	99·56
mg-no.	0·42	0·32	0·27	0·31	0·52	0·54	0·50	0·50	0·56	0·48	0·48	0·39	0·50	0·34	0·52
LOI	2·14	1·76	1·59	1·70	1·05	1·07	0·78	1·20	0·15	2·18	0·62	2·61	0·76	0·30	1·38
Ni	6	5	7	3	15	17	11	13	62	27	9	14	16	5	20
Cr	13	6	20	8	21	53	20	24	173	32	13	25	46	6	58
V	81	101	68	14	274	280	324	255	235	235	193	167	116	65	135
Sc	13	15	12	4	27	33	42	29	27	27	24	22	20	10	17
Cu	19	13	8	1	77	31	46	23	144	74	26	65	23	5	38
Zn	69	53	46	63	81	93	82	90	92	86	78	71	84	94	69
Ga	17	17	17	16	19	19	17	19	19	20	19	18	20	20	19
Pb	4·9	4·8	6·3	7·5	4·8	11·2	4·8	7·1	17·1	9·9	6·0	11·9	11·5	13·6	15·5
Sr	289	283	290	296	319	448	295	462	269	481	264	250	337	364	303
Rb	49·6	31·9	25·8	44·3	22·6	38·7	20·9	39·9	76·2	52·2	31·8	72·3	62·7	66·9	133
Ba	190	149	177	188	331	224	161	244	427	442	209	350	292	324	617
Zr	137	108	118	171	80	102	80	111	199	112	119	175	152	227	211
Nb	6·7	5·3	6·0	7·7	3·6	5·8	4·1	6·6	10·8	8·0	6·3	8·5	9·0	10·3	12·0
Th	3·6	3·0	2·7	3·7	2·6	3·7	2·1	3·2	9·5	4·0	3·3	7·0	4·8	10·5	15·2
Y	21·2	16·0	13·4	14·9	23·7	28·4	24·4	29·7	30·5	24·0	26·1	30·5	29·3	33·3	25·6
La	14	11	14	16	14	14	7	14	26	21	11	20	21	35	35
Ce	26	24	26	31	29	30	18	34	54	44	28	40	39	73	68
Nd	14	11	12	15	16	17	12	18	26	24	15	20	21	31	30
Major phases	plag, amph, (opx)	plag, amph, qz	plag, amph, (bi)	plag, amph, qz	plag, cpx, ol	plag, cpx, ol	plag, ol, cpx	plag, ol, cpx	plag, ol, cpx	plag, ol, cpx	plag, cpx, opx	plag, opx, cpx	plag, amph, gt	plag	plag, cpx, opx (amph)
Long.	25°16′	25°18′	25°21′	25°22′	25°15′	25°09′	25°21′	25°23′	25°24′	25°20′	25°25′	25°11′	25°12′	25°24′	25°21′
Lat.	47°03′	47°03′	47°03′	47°03′	47°03′	47°08′	47°05′	47°12′	46°58′	47°03′	47°08′	46°58′	47°13′	47°06′	47°05′

	Călimani				Gurghiu										
Sample:	C9	C14	C13	C16	G31	G12	G5	G1	G7	G19	G32	G39	G40	G3	G9
SiO_2	62·16	63·52	63·57	70·98	54·04	54·97	56·82	56·83	57·86	57·86	57·87	58·78	59·03	59·38	61·23
Al_2O_3	16·94	17·18	16·32	17·48	18·49	18·70	18·70	18·71	18·13	18·08	17·93	18·37	18·12	18·08	16·91
Fe_2O_3	4·81	4·73	4·80	1·03	7·87	8·70	7·47	7·29	7·39	6·85	6·84	6·39	6·82	6·47	6·04
MgO	3·31	2·54	3·89	0·22	4·79	4·23	3·32	3·86	3·38	3·26	3·62	3·01	3·42	3·19	3·11
CaO	5·64	5·58	5·08	3·08	9·69	8·31	7·79	7·93	7·41	7·35	7·18	6·92	6·97	6·95	6·32
Na_2O	3·74	3·11	3·65	3·85	3·19	2·96	3·53	3·35	3·55	3·65	3·63	3·53	3·72	3·49	3·50
K_2O	2·12	2·40	2·24	3·22	0·781	1·166	1·201	1·144	1·328	1·340	1·438	1·570	1·190	1·380	1·804
TiO_2	0·546	0·540	0·598	0·250	1·069	0·967	0·889	0·791	0·954	0·841	0·819	0·688	0·791	0·663	0·725
MnO	0·098	0·130	0·095	0·016	0·165	0·166	0·173	0·158	0·144	0·141	0·130	0·137	0·143	0·145	0·134
P_2O_5	0·177	0·192	0·182	0·127	0·142	0·145	0·201	0·155	0·202	0·146	0·185	0·154	0·127	0·168	0·163
Total	99·54	99·92	100·42	100·25	100·22	100·31	100·09	100·22	100·35	99·52	99·64	99·55	100·33	99·91	99·94
mg-no.	0·58	0·52	0·62	0·30	0·55	0·49	0·47	0·51	0·48	0·49	0·51	0·48	0·50	0·50	0·50
LOI	0·66	2·21	0·54	1·30	0·08	0·28	0·76	0·20	0·46	0·59	0·37	0·35	0·53	0·27	0·62
Ni	47	17	67	4	19	8	10	6	11	8	14	12	9	6	20
Cr	120'	38	160	3	89	17	15	10	7	13	30	14	14	9	54
V	91	101	90	20	296	248	176	170	179	176	162	136	158	136	136
Sc	15	13	13	4	40	31	21	20	23	22	21	18	22	18	19
Cu	34	41	23	0	54	23	44	25	65	32	33	79	23	21	20
Zn	62	85	54	46	96	82	77	78	71	68	75	67	81	70	66
Ga	18	18	18	21	19	19	18	19	20	18	19	19	17	18	17
Pb	12·8	12·4	11·5	22·4	5·1	10·1	4·8	4·3	3·3	8·8	7·3	5·7	4·4	6·5	7·7
Sr	391	323	366	299	343	283	274	281	301	236	322	316	234	290	244
Rb	62·6	154	79·6	124	17·6	37·2	36·8	33·7	39·7	42·7	45·6	49·6	37·1	40·8	59·9
Ba	569	380	582	676	152	206	302	279	348	314	429	394	264	334	448
Zr	140	170	141	165	92	104	137	117	159	137	151	153	129	132	154
Nb	8·6	9·5	10·3	14·6	4·2	6·4	8·5	5·6	11·7	6·7	9·7	8·2	6·4	6·8	11·7
Th	7·7	8·5	10·2	10·1	1·7	3·3	4·9	4·4	6·6	4·6	7·0	5·7	3·8	5·4	10·5
Y	15·8	27·8	16·7	12·2	27·0	25·2	29·0	23·0	25·1	22·8	23·2	21·3	23·4	22·3	21·9
La	24	24	26	26	9	13	19	17	22	14	27	22	14	17	24
Ce	45	46	49	51	18	28	36	33	43	28	49	42	29	34	45
Nd	19	24	21	24	12	15	19	17	21	15	21	19	14	17	20
Major phases	plag, cpx, opx amph, ol	plag, opx, cpx	plag, bi, amph, cpx, opx	plag, bi, qz	plag, cpx, opx (ap)	plag, cpx, opx	plag, cpx, opx	plag, cpx, opx	plag, cpx, opx	plag, cpx, opx	plag, cpx, opx (amph)	plag, cpx, opx	plag, cpx, opx amph	plag, cpx, opx amph	plag, amph cpx, opx
Long.	25°19′	25°13′	25°13′	25°25′	24°57′	24°57′	25°24′	25°33′	25°19′	25°12′	25°11′	25°29′	25°25′	25°26′	25°22′
Lat.	46°57′	47°17′	47°06′	47°11′	46°35′	46°54′	46°36′	46°37′	46°40′	46°49′	46°37′	46°35′	46°34′	46°37′	46°44′

(continued on next page)

Table 2: continued

	Northern Harghita												
Sample:	H51	H21	H17	H23	H20	H30	H8	H18	H24	H27	H16	H44	H28
SiO_2	56·02	57·90	59·06	60·18	60·60	60·94	61·85	62·31	63·15	65·88	65·95	67·75	69·93
Al_2O_3	18·38	18·86	18·43	17·85	16·94	17·62	17·61	18·86	16·88	17·01	16·80	16·99	15·98
Fe_2O_3	6·80	7·16	6·29	5·99	5·88	5·76	5·18	5·22	4·80	4·58	4·04	4·04	3·15
MgO	3·94	3·20	3·32	3·40	3·64	3·07	3·12	2·73	2·91	0·79	2·81	0·10	0·34
CaO	8·92	6·91	6·49	6·71	6·88	6·25	5·80	5·43	5·99	3·79	3·95	3·72	2·82
Na_2O	3·13	3·50	3·47	3·56	2·82	3·23	3·05	3·11	3·46	4·68	2·88	4·52	4·28
K_2O	1·219	1·416	1·810	1·736	2·17	2·07	2·11	1·940	1·98	2·26	2·55	2·64	2·83
TiO_2	0·860	0·741	0·732	0·617	0·700	0·641	0·689	0·646	0·531	0·556	0·537	0·441	0·281
MnO	0·135	0·139	0·109	0·159	0·124	0·120	0·098	0·112	0·104	0·076	0·083	0·029	0·097
P_2O_5	0·151	0·204	0·141	0·128	0·134	0·127	0·137	0·144	0·120	0·224	0·092	0·168	0·113
Total	99·65	100·02	99·85	100·32	99·87	99·83	99·65	100·49	99·92	99·83	99·68	100·39	99·82
mg-no.	0·54	0·47	0·51	0·53	0·55	0·51	0·54	0·51	0·55	0·26	0·58	0·05	0·18
LOI	1·84	0·69	1·06	0·97	0·50	0·48	1·41	2·18	0·48	1·03	2·07	1·03	1·13
Ni	7	5	7	18	8	6	12	6	14	3	19	4	3
Cr	37	11	16	30	94	19	56	15	37	9	80	4	4
V	101	85	146	126	73	106	74	56	80	33	56	26	8
Sc	26	18	21	21	17	16	18	16	15	8	17	5	2
Cu	9	7	11	17	15	8	6	8	17	13	16	6	5
Zn	71	75	61	60	69	65	61	62	57	79	50	65	66
Ga	18	19	18	18	19	18	19	19	16	18	17	17	16
Pb	4·6	6·2	7·5	6·1	11·1	9·0	12·1	11·0	8·7	12·6	11·9	12·2	13·0
Sr	372	469	337	324	374	376	308	317	317	274	223	305	241
Rb	41·9	42·3	63·3	63·1	87·1	75·9	79·6	77·9	78·3	81·3	102	95·2	108
Ba	299	390	522	408	509	408	496	475	484	548	532	502	565
Zr	125	146	148	148	143	149	149	143	137	211	141	204	218
Nb	11·6	10·6	10·7	8·3	12·7	8·1	12·6	11·4	8·8	12·4	10·6	9·2	9·0
Th	4·3	7·0	8·9	8·1	11·0	9·7	11·0	10·0	9·6	11·1	12·9	11·0	12·1
Y	21·7	23·7	26·9	22·0	26·1	20·6	21·5	21·2	21·0	24·8	20·3	18·2	14·9
La	17	26	25	20	30	24	25	25	26	35	27	27	28
Ce	34	49	45	37	53	41	45	46	42	53	46	49	45
Nd	17	21	20	17	23	18	19	19	18	26	18	20	17
Major phases	plag, cpx	plag, opx, cpx amph	plag, opx, cpx	plag, cpx, opx	plag, opx, cpx bi, amph	plag, amph, cpx, opx	plag, cpx, opx amph	plag, opx, cpx amph	plag, cpx, opx	plag, amph	plag, amph, cpx, qz	plag	plag, amph
Long.	25°40′	25°40′	25°44′	25°39′	25°41′	25°35′	25°51′	25°42′	25°41′	25°40′	25°48′	25°38′	25°40′
Lat.	46°06′	46°22′	46°08′	46°23′	46°20′	46°34′	46°21′	46°22′	46°25′	46°27′	46°18′	46°32′	46°36′

JOURNAL OF PETROLOGY VOLUME 37 NUMBER 4 AUGUST 1996

	Southern Harghita									
Sample:	H11	H2	H3	H13	H4	H12	H45	H7	H10	H6
SiO_2	54·90	57·49	58·05	59·51	59·72	63·16	64·48	64·61	67·97	68·45
Al_2O_3	18·54	15·90	15·77	17·69	17·77	17·51	16·63	17·58	16·40	16·27
Fe_2O_3	7·59	6·09	4·90	5·71	5·16	4·27	4·48	2·53	2·56	2·07
MgO	3·70	4·29	4·49	2·93	3·59	2·18	3·12	1·88	1·66	1·38
CaO	8·24	7·21	6·76	6·22	6·01	4·92	4·93	4·49	3·51	2·96
Na_2O	3·72	3·85	3·92	3·86	4·03	4·38	2·99	4·64	4·40	4·88
K_2O	1·613	3·32	4·04	1·902	2·18	2·58	2·44	3·25	3·38	3·58
TiO_2	1·018	0·892	0·967	0·767	0·798	0·586	0·550	0·526	0·377	0·304
MnO	0·193	0·134	0·085	0·111	0·090	0·101	0·097	0·047	0·060	0·050
P_2O_5	0·168	0·339	0·516	0·179	0·173	0·197	0·108	0·192	0·143	0·127
Total	99·68	99·52	99·50	99·88	99·52	99·88	99·81	99·75	100·45	100·08
mg-no.	0·49	0·58	0·65	0·50	0·58	0·50	0·58	0·60	0·58	0·57
LOI	1·78	1·92	0·56	0·70	0·69	1·35	1·44	0·61	1·76	1·56
Ni	18	42	36	11	18	7	30	7	14	14
Cr	40	147	124	21	53	13	62	14	22	22
V	203	123	115	129	134	81	60	66	49	39
Sc	27	16	14	18	18	11	15	10	6	5
Cu	31	56	18	12	18	7	14	11	4	5
Zn	70	62	54	53	49	41	58	39	38	37
Ga	19	18	19	17	19	18	18	19	17	19
Pb	22·6	18·5	23·1	11·1	22·0	15·6	12·5	17·4	25·0	30·8
Sr	948	1540	2264	558	1181	871	754	1266	1028	1319
Rb	35·1	53·5	65·8	58·9	53·2	70·2	85·4	83·3	98·8	88·2
Ba	541	1372	2695	676	876	1128	572	1461	1250	1241
Zr	108	184	235	123	125	124	143	146	132	122
Nb	11·8	19·9	18·7	14·8	14·4	20·3	9·1	17·4	14·9	11·8
Th	5·0	8·6	14·0	11·3	8·2	13·3	11·3	12·5	15·2	13·4
Y	25·6	15·9	18·5	18·6	17·5	15·7	16·5	13·7	11·5	8·4
La	20	48	101	31	28	38	25	41	33	29
Ce	37	91	195	52	50	64	45	70	57	48
Nd	17	38	82	20	22	23	19	25	20	18
Major phases	plag, ol, cpx, opx	ol, cpx, amph, bi qz, plag	cpx, opx kfeld, bi amph sp	plag, cpx, opx (ol)	plag, amph, bi cpx, opx	plag, amph, bi	plag, bi, amph cpx, opx	plag, amph, bi kfeld	plag, bi amph qz kfeld sp	plag, amph, bi
Long.	25°49′	25°49′	25°49′	25°48′	25°51′	25°48′	25°50′	25°58′	25°55′	25°54′
Lat.	46°10′	46°03′	46°04′	46°03′	46°07′	46°09′	46°23′	46°07′	46°11′	46°07′

(continued on next page)

Table 2: continued

	Local metamorphic basement						Paleo-accretionary wedge sediments							
Sample:	CB1	CB3	CB4	CB5	CB6	CB7	FS1	FS2	FS3	FS4	FS6	FS7	FS8	FS9
Series:	Negris.	Bretila	Negris.	Bretila	Rebra	Negris.	Ceahlau	Ceahlau	Convol.	Convol.	Ceahlau	Margin.	Tarcau	SubCarp
SiO_2	68·01	65·75	67·97	90·03	64·89	61·20	59·99	28·28	57·22	58·22	58·66	60·36	70·84	60·88
Al_2O_3	16·32	16·05	14·59	5·99	19·30	20·08	18·31	4·56	20·02	15·82	17·53	10·47	18·94	20·33
Fe_2O_3	5·98	5·62	5·61	0·91	7·35	7·47	10·84	3·44	8·73	5·64	5·62	4·84	3·51	6·20
MgO	2·41	2·30	1·75	0·10	2·29	2·57	2·45	1·33	3·70	2·90	2·79	1·80	1·83	2·98
CaO	0·95	4·86	2·53	0·05	0·49	0·40	0·48	60·33	3·66	11·61	9·72	19·44	0·12	3·90
Na_2O	2·32	3·20	2·95	1·88	1·45	1·91	0·75	0·49	1·13	1·27	1·69	1·03	0·65	1·15
K_2O	2·80	1·900	3·14	1·009	3·18	5·00	5·62	0·490	4·13	3·24	3·33	1·798	3·56	4·03
TiO_2	0·767	0·583	0·758	0·152	0·806	1·031	0·903	0·175	0·925	0·709	0·898	0·557	0·923	0·766
MnO	0·107	0·102	0·081	0·026	0·111	0·085	0·255	0·542	0·057	0·119	0·050	0·097	0·009	0·098
P_2O_5	0·182	0·090	0·178	0·040	0·133	0·192	0·110	0·073	0·144	0·171	0·170	0·159	0·076	0·131
Total	99·83	100·45	99·55	100·19	100·00	99·94	99·71	99·71	99·72	99·70	100·45	100·50	100·45	100·45
mg-no.	0·42	0·42	0·36	0·16	0·36	0·38	0·29	0·41	0·43	0·48	0·47	0·40	0·48	0·46
LOI	3·17	2·11	3·10	1·89	2·66	2·21	2·10	2·87	1·90	2·22	2·71	2·80	2·99	3·22
Ni	45	10	21	11	44	54	128	45	75	49	85	41	23	77
Cr	94	29	50	11	108	120	114	28	141	101	151	70	152	157
V	128	120	91	18	133	164	174	36	183	135	160	93	225	202
Sc	17	19	17	1	17	21	22	0	24	19	19	10	19	22
Cu	21	12	13	1	43	27	37		63	36	43	6	19	46
Zn	89	68	91	16	210	127	145	24	163	120	134	44	44	122
Ga	19	17	18	7	28	25	23	6	25	19	21	10	23	26
Pb	15·1	11·5	17·7	7·9	9·2	8·6	43·0	6·7	27·6	28·5	20·2	5·0	13·2	19·4
Sr	87	145	207	18	105	86	35	1018	103	204	352	270	71	187
Rb	77·1	66·1	106	27·1	113	169	248	22·1	195	139	145	65·6	150	187
Ba	732	322	888	315	578	1011	383	83	640	467	413	998	319	389
Zr	189	125	258	58	197	207	179	23	204	157	223	188	233	127
Nb	13·6	6·9	15·4	3·4	13·7	18·3	17·7	3·6	17·0	13·4	17·5	9·8	16·7	16·1
Th	9·8	5·3	14·8	3·3	12·0	13·7	12·5	2·7	15·8	10·4	13·2	7·2	8·9	12·8
Y	25·5	34·7	37·0	8·9	28·7	30·6	26·3	28·1	36·8	40·1	24·3	31·0	21·6	26·5
La	34	17	42	12	36	28	19	18	37	32	36	27	29	37
Ce	68	36	88	21	73	67	47	33	81	70	73	54	57	77
Nd	31	19	40	9	33	26	19	20	37	31	32	28	24	33

Analyses were calculated on a volatile-free basis with major elements given in wt% and trace elements in p.p.m. Reproducibility is reported in the text. Additional data are available from the authors on request. Dominant phenocryst phases present in each rock are indicated in the table using the following notation: plag, plagioclase; cpx, clinopyroxene; opx, orthopyroxene; ol, olivine; amph, amphibole; bi, biotite; qz, quartz; ap, apatite; kfeld, sanidine; sp, sphene; gt, garnet. Parentheses indicate that the mineral in question is rare. Sampling localities are given with reference to latitude and longitude.

Table 3: Sr–Nd–Pb–O isotope analyses for representative CGHA volcanic and crustal rocks

	$^{87}Sr/^{86}Sr$	$^{143}Nd/^{144}Nd$	ε_{Nd}	$^{206}Pb/^{204}Pb$	$^{207}Pb/^{204}Pb$	$^{208}Pb/^{204}Pb$	$\Delta^{207}Pb$	$\Delta^{208}Pb$	$\delta^{18}O_{opx}$	$\delta^{18}O_{other}$	
Low-K Călimani											
C2	0·70419±1	0·512868±4	4·3	18·819	15·627	38·737	9·6	36		6·0 (plag)	5·4 (amph)
C3	0·70450±1	0·512815±5	3·2								
C7	0·70457±1	0·512780±9	2·6	18·775	15·634	38·737	10·8	41		5·2(amph)	
C8	0·70409±1	0·512902±5	4·9	18·834	15·641	38·748	10·8	35		5·1 (amph)	
Călimani											
C1	0·70686±1	0·512646±6	−0·6	18·904	15·661	38·925	12·1	44	5·9	5·7 (ol)	
C4	0·70552±2	0·512775±4	2·5	18·821	15·644	38·823	11·3	44	5·8		
C5	0·70995±1	0·512448±5	−3·9	18·889	15·656	38·937	11·7	47	7·3		
C6	0·70673±1	0·512494±5	−3·0	18·762	15·650	38·847	12·5	54	7·0		
C9	0·70863±2	0·512494±5	−3·0	18·797	15·650	38·978	12·1	63			
C10	0·70664±1	0·512651±5	0·0	18·821	15·661	38·895	13·0	51	5·7		
C13	0·70902±1	0·512391±5	−5·0	18·820	15·644	38·932	11·3	55			
C14	0·70694±1	0·512572±5	−1·5								
C16	0·71028±1	0·512473±4	−3·4	18·978	15·667	38·953	11·9	38		8·7 (bi)	
C18	0·70651±1	0·512588±5	−1·0								
C21	0·70830±1	0·512494±11	−3·0	18·986	15·679	38·973	13·0	39			
C24	0·70620±1	0·512565±13	−1·6								
C26	0·70752±1	0·512520±9	−2·5	18·980	15·675	38·956	12·7	38		7·6 (amph)	7·4 (gt)
C47	0·70609±1	0·512571±6	−1·5	18·872	15·663	38·924	12·6	48	6·7		
C65	0·70525±1	0·512749±5	2·0	18·858	15·668	38·941	13·3	52	5·6		
Gurghiu											
G1	0·70627±1	0·512654±5	0·1	18·903	15·673	39·070	13·3	59	6·4		
G3	0·70620±2	0·512621±5	−0·6	18·951	15·682	39·108	13·7	57	6·0		
G5	0·70603±1	0·512617±5	−0·6								
G7	0·70547±2	0·512720±8	1·4	18·898	15·650	39·046	11·1	57	5·7		
G9	0·70657±1	0·512592±4	−0·9								
G12	0·70745±1	0·512499±5	−2·9						6·2		
G19	0·70557±1	0·512711±13	1·2								
G31	0·70508±1	0·512703±9	1·1	18·794	15·654	38·790	12·6	44	5·7		
G32	0·70820±1	0·512413±7	−4·6	18·784	15·656	38·933	12·9	60	5·9	5·7 (amph)	
G39	0·70669±1	0·512563±5	−1·7								
G40	0·70565±1	0·512689±5	0·8								

(continued on next page)

Table 3: continued

	$^{87}Sr/^{86}Sr$	$^{143}Nd/^{144}Nd$	ε_{Nd}	$^{208}Pb/^{204}Pb$	$^{207}Pb/^{204}Pb$	$^{208}Pb/^{204}Pb$	$\Delta^{207}Pb$	$\Delta^{208}Pb$	$\delta^{18}O_{opx}$	$\delta^{18}O_{other}$	
Northern Harghita											
H8	0·70690 ± 1	0·512444 ± 5	−4·0	18·990	15·691	39·093	14·2	51	8·5	8·5 (amph)	
H16	0·70690 ± 1	0·512471 ± 5	−3·5	18·981	15·696	39·086	14·8	51			
H17	0·70577 ± 1	0·512612 ± 11	−0·7								
H18	0·70681 ± 2	0·512487 ± 5	−3·2	19·014	15·683	39·134	13·1	52		7·8 (amph)	8·3 (opx)
H_20	0·70719 ± 1	0·512407 ± 5	−4·7	19·037	15·692	39·123	13·7	48	8·0	7·6 (amph)	
H_21	0·70679 ± 1	0·512567 ± 9	−1·6								
H_23	0·70584 ± 1	0·512534 ± 5	−2·2								
H_24	0·70636 ± 1	0·512532 ± 6	−2·3	18·878	15·661	38·973	12·4	52	7·7	7·4 (opx)	
H_27	0·70558 ± 1	0·512637 ± 9	−0·2	18·881	15·674	39·028	13·6	57		7·0 (opx)	
H_28	0·70622 ± 1	0·512644 ± 6	−0·1								
H30	0·70664 ± 1	0·512478 ± 4	−3·3								
H44	0·70598 ± 1	0·512610 ± 6	−0·8								
H51	0·70624 ± 1	0·512507 ± 5	−2·8								
Southern Harghita											
H_2	0·70478 ± 1	0·512632 ± 4	−0·3	18·603	15·703	39·243	19·5	113	7·1		
H3	0·70464 ± 1	0·512626 ± 5	−0·5	18·574	15·660	38·785	15·6	70	6·9		
H4	0·70502 ± 1	0·512532 ± 5	−2·3	18·578	15·664	38·723	15·9	64	6·9		
H6	0·70485 ± 1	0·512477 ± 4	−3·4	18·427	15·649	38·701	16·1	80		6·3 (bi)	7·3 (plag)
H7	0·70569 ± 1	0·512409 ± 5	−4·7								
H10	0·70551 ± 1	0·512454 ± 5	−3·8	18·474	15·683	39·014	18·9	105		6·6 (amph)	6·6 (bi)
H11	0·70478 ± 1	0·512623 ± 5	−0·5	18·612	15·644	38·578	13·6	45	6·4		
H12	0·70544 ± 1	0·512542 ± 6	−2·1								
H13	0·70623 ± 1	0·512440 ± 8	−4·1	18·754	15·733	39·498	20·9	120	6·4	6·8 (opx)	
H45	0·70491 ± 1	0·512481 ± 5	−3·3								

JOURNAL OF PETROLOGY VOLUME 37 NUMBER 4 AUGUST 1996

	$^{87}Sr/^{86}Sr$	$^{143}Nd/^{144}Nd$	ε_{Nd}	$^{206}Pb/^{204}Pb$	$^{207}Pb/^{204}Pb$	$^{208}Pb/^{204}Pb$	$\Delta^{207}Pb$	$\Delta^{208}Pb$	$\delta^{18}O_{cpx}$	$\delta^{18}O_{WR}$
Southern back-arc calc-alkaline										
Rupea	0·70407 ± 1*	0·512760 ± 40*	2·2	18·628	15·592	38·503	8·2	36	5·9	
Lgf	0·70441 ± 1*	0·512762 ± 6*	2·2	18·578	15·630	38·418	12·5	33		
Local metamorphic basement										
CB1	0·72136 ± 1	0·512057 ± 9	−11·5	18·381	15·676	38·713	19·3	86		
CB3	0·70936 ± 1	0·512348 ± 5	−5·9	18·710	15·633	38·614	11·4	37		
CB4	0·71839 ± 1	0·512134 ± 5	−10·0	18·458	15·679	38·730	18·7	79		17·9
CB5	0·72431 ± 2	0·512295 ± 6	−6·9	18·543	15·637	38·570	13·6	53		
CB6	0·73201 ± 1	0·511963 ± 5	−13·4	19·236	15·767	39·837	19·1	95		13·1
CB7	0·73619 ± 1	0·512067 ± 9	−11·4	19·352	15·736	39·781	14·7	76		
Paleo-accretionary wedge sediments										
FS1	0·75007 ± 1	0·512246 ± 15	−7·6							
FS2	0·70780 ± 1	0·512242 ± 6	−7·7	18·634	15·651	38·724	14·0	57		
FS3	0·72740 ± 1	0·512126 ± 4	−10·0	18·642	15·654	38·753	14·2	59		
FS4	0·71562 ± 1	0·512141 ± 5	−9·7	18·616	15·685	38·811	17·6	68		
FS6	0·71171 ± 1	0·512147 ± 4	−9·6	18·775	15·663	38·897	13·7	57		
FS7	0·71024 ± 1	0·512255 ± 6	−7·5	18·895	15·665	38·731	17·4	78		
FS8	0·72337 ± 1	0·512127 ± 5	−10·0	19·012	15·667	39·185	11·5	57		
FS9	0·71556 ± 1	0·512186 ± 4	−8·8	18·826	15·654	38·753	12·2	37		

ε_{Nd} is reported relative to a CHUR value of 0·512638. $\Delta^{207}Pb$ and $\Delta^{208}Pb$ have been calculated using the NHRL of Hart (1984). Errors quoted are the internal precision at 2 SE for Sr and Nd isotope analyses. Internal error on Pb isotope determinations is insignificant when SRM 981 reproducibility is taken into consideration.
*Analyses taken from Downes *et al.* (1995*b*).

Xenoliths of crustal material, typically schists and gneisses, are common within the lava flows. Cognate plutonic xenoliths with igneous textures, composed of amphibole ± clinopyroxene ± plagioclase ± magnetite, are also widespread as are basic and acidic igneous inclusions. Xenoliths of older andesite are sometimes found. However, lower-crustal and mantle xenoliths are not found in CGHA lavas.

MAJOR AND TRACE ELEMENT GEOCHEMISTRY

Major element variations

Most CGHA samples are medium-K calc-alkaline to high-K calc-alkaline and are andesitic and dacitic in character (Fig. 2). A few lavas have low-K signatures, although tholeiitic volcanism is absent. Basalts are rare and occur only in the Călimani centre; rhyodacites are also rare, although evolved differentiation products may occur within pyroclastic flows where poor preservation precludes sampling for geochemical study.

CGHA magmatic rocks have been divided into five groups using the criteria of age, occurrence and chemistry (Table 1). The Low-K Călimani group (~1% K_2O) consists of four evolved rocks (62–68% SiO_2) from the south-east of the Călimani centre. These are close to the base of the volcanic pile and have K/Ar ages in the range 8·6–8·0 Ma, i.e. towards the earlier stages of Călimani volcanism (Pécskay *et al.*, 1995*a*). The Călimani group covers the widest range of compositions within the CGHA from basalt to rhyodacite (51–71% SiO_2). This is also the most voluminous lava sequence, including the bulk of the extrusive products in the Călimani volcanic centre. K_2O varies considerably within this group, from 0·6 to 3·2%. The Gurghiu group shows a moderately large compositional variation but does not extend above 64% SiO_2 or 2·0% K_2O. Northern Harghita group lavas are generally evolved (57–70% SiO_2) and cover a narrow band of variation in the medium-K calc-alkaline field. Southern Harghita group centres, in the extreme south of the CGHA, are more potassic and overlap the shoshonitic field. There is a general increase in K_2O content of the lavas at a constant SiO_2 content, through volcanic centres, southwards from the Gurghiu Mountains to the Southern Harghita

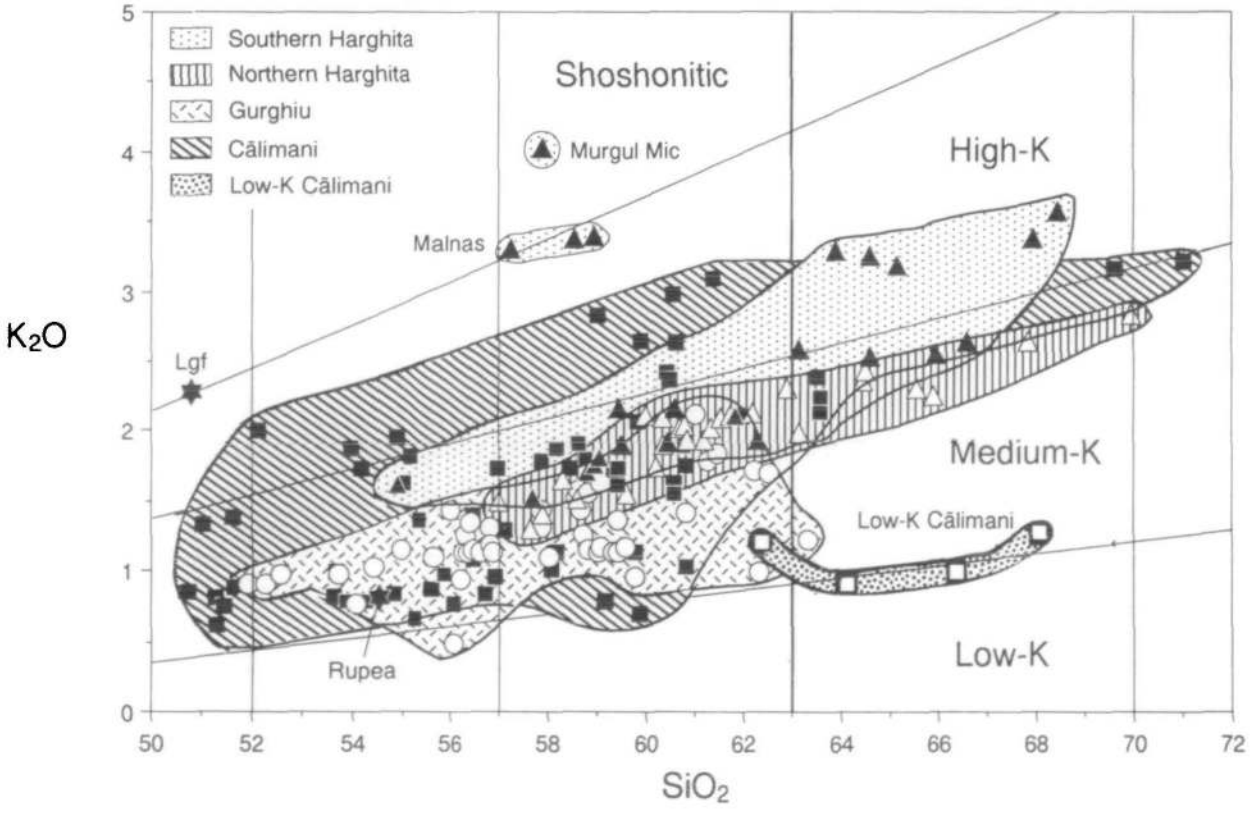

Fig. 2. SiO_2 vs K_2O diagram of Gill (1981) for CGHA rocks. Symbols are as follows: filled squares, Călimani; open squares, Low-K Călimani; open circles, Gurghiu; open triangles, Northern Harghita; filled triangles, Southern Harghita; filled stars, Rupea and La Gruiu Fintina. Data from Rupea and La Gruiu Fintina are taken from Downes *et al.* (1995*b*).

Mountains. This mirrors a general decrease in the age of the rocks.

The back-arc basaltic andesite from Rupea (Downes *et al.*, 1995*b*) has characteristics similar to magmas in the Gurghiu group. The block from La Gruiu Fintina plots on the boundary between the basalt and absarokite fields (Fig. 2) and is close in composition to the high-K rocks of the Southern Harghita group.

Major elements show clear trends within most volcanic centres and within the spatial and temporal groups defined above (Fig. 3). MgO, CaO, Fe_2O_3, TiO_2, MnO and P_2O_5 display negative correlations with SiO_2, whereas K_2O and Na_2O increase with increasing SiO_2. These trends are consistent with fractional crystallization involving olivine and clinopyroxene in the most basic magmas (supported by a steep trend on MgO vs SiO_2 for Călimani basaltic rocks). Clinopyroxene, orthopyroxene, plagioclase, amphibole, apatite, magnetite and ilmenite fractionated in the intermediate magmas, with the additional effect of biotite in the more fractionated and high-K magmas of the Southern Harghita group (Mason *et al.*, 1995). Fractionation of amphibole, pyroxene, plagioclase and magnetite is indicated by the widespread presence of cognate xenoliths which contain these phases.

Some of the scatter in major element variation diagrams may be due to magma mixing. A high-K magma H3 from the shoshonitic lava dome of Murgul Mic contains very high P_2O_5 and low Al_2O_3 (Table 2). This rock contains a disequilibrium mineral assemblage with coexisting olivine, pyroxene, quartz, amphibole and biotite phenocrysts. Similarly, an olivine- and amphibole-bearing andesite (C13) from Călimani shows anomalously high MgO. Both Na and Al show much more scatter than the other major elements, a feature which may be attributable to variable fractionation and mixing, probably involving plagioclase. Crustal wall-rock assimilation may also have affected major element concentrations (Mason *et al.*, 1995).

Trace element signatures

Ni and Cr generally behaved compatibly in the most basic magmas and have low concentrations in even the most basic magmas (Fig. 3; Table 2), supporting the assertion that a large amount of fractionation of olivine and the pyroxenes occurred at an early stage. Some andesites have high Ni contents owing to the presence of olivine- and clinopyroxene-rich basic inclusions or xenocrysts. Sc was removed from the melt by fractionation of pyroxenes, amphibole and Fe–Ti oxides. Y was compatible in amphibole (hornblende), which is a ubiquitous phenocryst in more evolved rocks. Sr contents are considerably elevated in the Southern Harghita group (800–2695 p.p.m.) but on a smaller scale there is a large variation between 300 and 450 p.p.m. in the Călimani group basalts. Sr remains relatively constant with increasing SiO_2, indicating control by the fractionation of plagioclase in shallow crustal magma chambers (Mason *et al.*, 1995).

Figure 4 shows normal mid-ocean ridge basalt (N-MORB) normalized (Sun & McDonough, 1989) incompatible trace element diagrams for representative samples from the CGHA and present-day subduction zones in the Mediterranean region. In general, LILE to HFSE ratios are high (e.g. Ba/Nb = 50) in CGHA lavas and a pronounced trough is seen at Nb which is typical for arc magmas. There is only a small enrichment in Nb and Zr and no enrichment in Ti above N-MORB concentrations but LREE and Pb contents are considerably elevated. Trace element patterns for CGHA basalts (Figs. 4a,d) are very similar to those from the Aeolian arc (Ellam *et al.*, 1988), which are considered to have been derived from a source enriched by sediment subduction, and the Aegean arc (Barton *et al.*, 1983), thought to be from a source enriched by sediment subduction and subsequently modified by intra-crustal contamination. A striking similarity is seen between trace element signatures for the arc volcanics and those for local crust and sediments (Fig. 4b).

Figure 4b shows data for representative andesites at 57% SiO_2 from each group of volcanic centres. This is the most basic composition at which magmas from each group can be compared. Trace element patterns are affected to some degree by fractional crystallization. Ti is depleted through the removal of magnetite and ilmenite, P by apatite and Sr by plagioclase. The Călimani, Gurghiu and Northern Harghita groups have very similar patterns, suggesting they have undergone fractionation involving common minerals from similar parental basalts. The Southern Harghita group differs by having elevated incompatible trace element concentrations which increase from moderate levels in the rest of the arc (e.g. ~300 p.p.m. Sr) to very high concentrations (1540–2695 p.p.m. Sr) in the high-K magmas. Most incompatible trace elements are enriched, including the LILE, LREE and HFSE, but the enrichment is not uniform, with fractionation of Ba/La, Ba/Rb and Sr/Y ratios reflecting an increase in Ba and Sr over the other incompatible elements. Rb, K, P, Ti and Y could have been removed by the fractionation of mineral phases which are present in some high-K Southern Harghita rocks, notably biotite, sphene

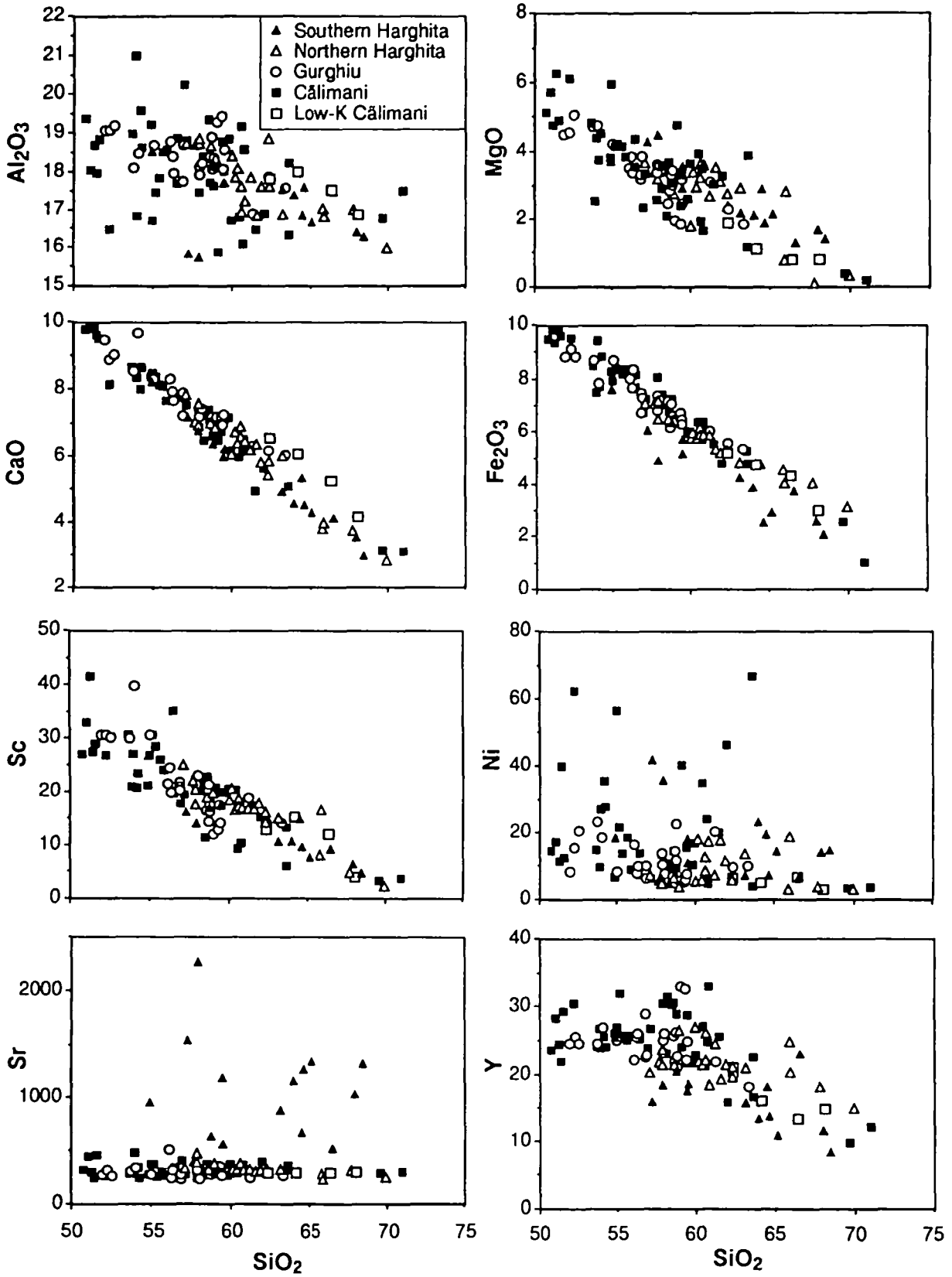

Fig. 3. Major and trace element Harker variation diagrams for CGHA lava suites. Symbols are as those in Fig. 2.

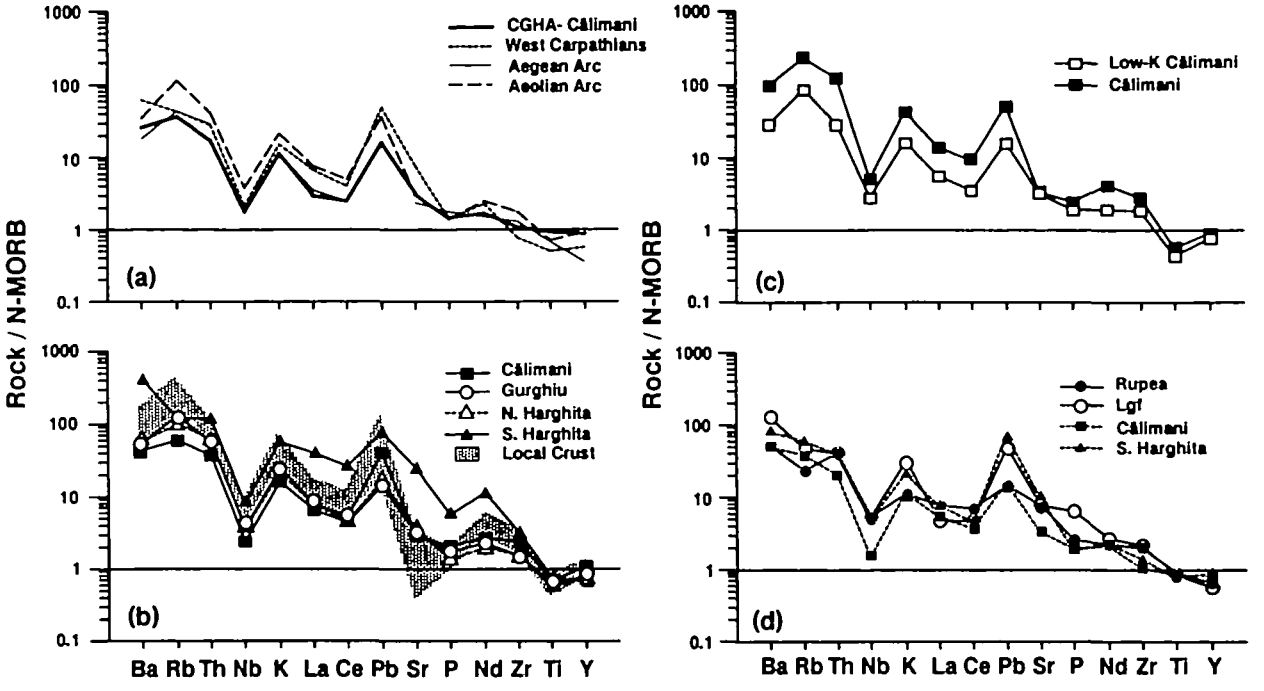

Fig. 4. N-MORB-normalized incompatible trace element diagrams using the normalizing coefficients of Sun & McDonough (1989). (a) Comparison of CGHA basalt data (C65) with other local arcs. Data sources are: Western Carpathians—Downes *et al.* (1995*a*); Aegean arc—Barton *et al.* (1983); Aeolian arc—Ellam *et al.* (1988). (b) Representative samples at 57% SiO_2 for the main groups of the CGHA. The field for upper-crustal samples and flysch sediments is also shown (local crust field). (c) Samples from the low-K Călimani and Călimani groups with 62% SiO_2. (d) Basalts from Călimani, the Southern Harghita group and back-arc calc-alkaline basalts.

and amphibole. However, Th and Pb would not be removed by fractionation of this assemblage and are not enriched to the same degree as Ba and Sr. Nb and Y contents are similar to other CGH lavas, precluding extensive sphene and amphibole removal. Thus, fractional crystallization combined with smaller degrees of partial melting does not explain the elevated Sr and Ba contents.

Figure 4c shows MORB-normalized incompatible element patterns for evolved andesites in both the main Călimani and the low-K Călimani groups. The patterns are similar in shape but the low-K Călimani pattern is significantly less enriched in all incompatible trace elements. The low-K rocks are also less enriched than more basic lavas from the rest of the arc.

Incompatible trace element concentrations (Fig. 4d) in the back-arc calc-alkaline sample from La Gruiu Fintina are very similar to those in a basaltic andesite from the Southern Harghita Mountains. In comparison, a basalt from Călimani has a slightly different trace element pattern with lower overall concentrations. The Rupea basaltic andesite has a much smaller positive Pb anomaly and lower Rb/Th than the other basaltic samples. There may be a close geochemical relationship between the La Gruiu Fintina high-K basalt and the Southern Harghita group, but the Rupea lava is different from all of the CGHA lavas.

ISOTOPE GEOCHEMISTRY

Sr–Nd–Pb isotopes

Values of $^{87}Sr/^{86}Sr$ and $^{143}Nd/^{144}Nd$ (Table 3, Fig. 5a) vary widely in the CGHA and reach strongly enriched compositions ($^{87}Sr/^{86}Sr = 0{\cdot}70409$–$0{\cdot}71028$; $^{143}Nd/^{144}Nd = 0{\cdot}512902$–$0{\cdot}512391$), overlapping the fields of the Aegean arc (Briqueu *et al.*, 1986) and the Aeolian arc (Ellam *et al.*, 1988). The Western Carpathian calc-alkaline arc (Salters *et al.*, 1988) defines a narrow Sr–Nd isotope field which reaches more enriched $^{87}Sr/^{86}Sr$ ratios than the CGHA trend.

The five groups defined in Table 1 are largely discriminated by their Sr–Nd isotope ratios (Fig. 5b). The low-K Călimani group has the lowest $^{87}Sr/^{86}Sr$ and highest $^{143}Nd/^{144}Nd$ for the CGHA whereas the Călimani group shows a large variation ($^{87}Sr/^{86}Sr = 0{\cdot}70525$–$0{\cdot}71028$; $^{143}Nd/^{144}Nd = 0{\cdot}512775$–$0{\cdot}512391$) and reaches the most enriched $^{87}Sr/^{86}Sr$ values. The Gurghiu group has intermediate isotope ratios ($^{87}Sr/^{86}Sr = 0{\cdot}70508$–$0{\cdot}70820$; $^{143}Nd/^{144}Nd = 0{\cdot}512720$–$0{\cdot}512413$) and is wholly enclosed within the Călimani field. Further south, the Northern Harghita ($^{87}Sr/^{86}Sr = 0{\cdot}70558$–$0{\cdot}70719$;

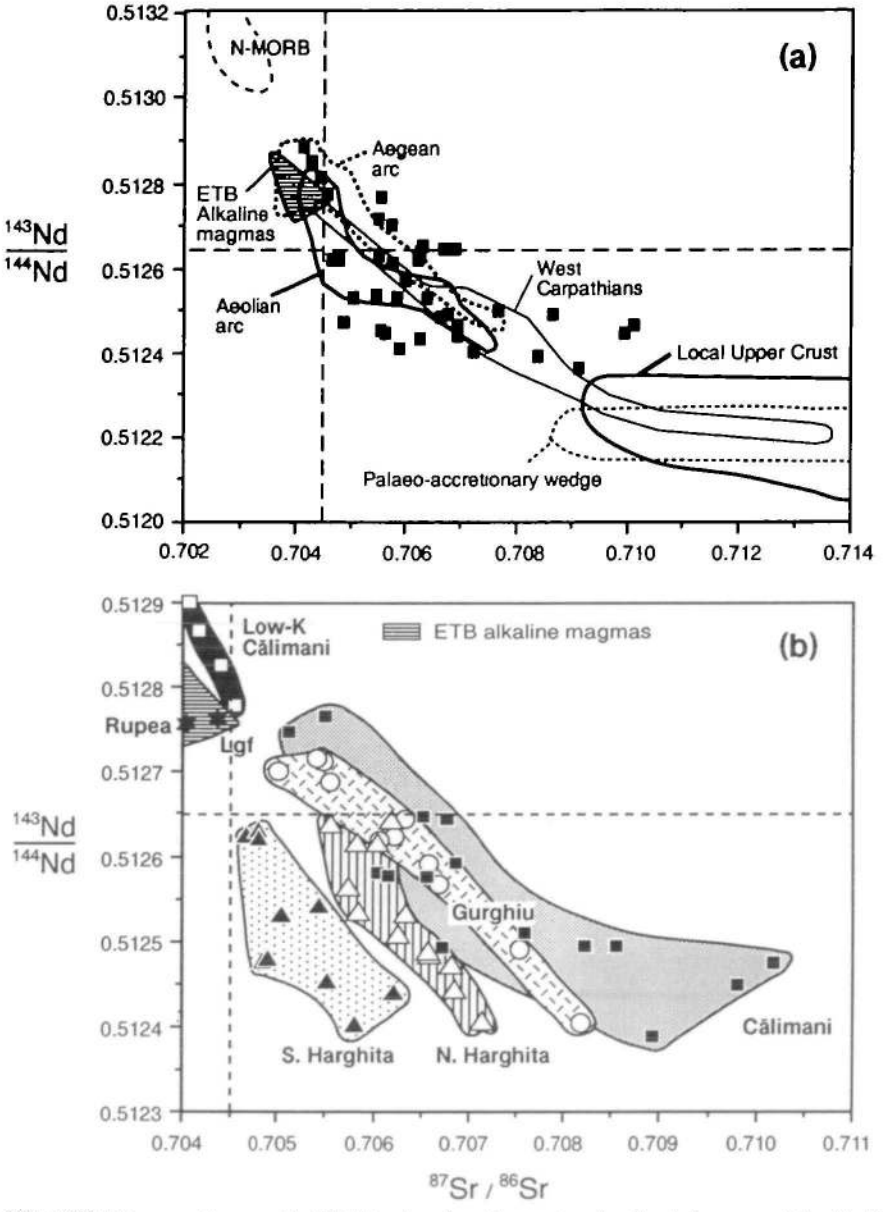

Fig. 5. $^{87}Sr/^{86}Sr$ vs $^{143}Nd/^{144}Nd$ isotope diagram for CGHA volcanic and crustal rocks. Symbols are explained in Fig. 2. (a) Comparison with other arc and mantle reservoirs in the Carpatho-Balkan–Mediterranean areas. Data sources are: West Carpathians—Salters *et al.* (1988); East Transylvanian Basin (ETB) alkali basalts—Downes *et al.* (1995*b*); Aeolian arc—Ellam *et al.* (1988); Aegean arc—Briqueu *et al.* (1986); N-MORB compilation of Saunders *et al.* (1988). (b) Variations within the CGHA. Progressing southwards from the Călimani group to the Southern Harghita group $^{87}Sr/^{86}Sr$ decreases at a constant $^{143}Nd/^{144}Nd$.

$^{143}Nd/^{144}Nd = 0{\cdot}512644$–$0{\cdot}512407$) and Southern Harghita groups ($^{87}Sr/^{86}Sr = 0{\cdot}70464$–$0{\cdot}70623$; $^{143}Nd/^{144}Nd = 0{\cdot}512632$–$0{\cdot}512409$) have slightly lower $^{87}Sr/^{86}Sr$. From north to south within the CGHA, $^{87}Sr/^{86}Sr$ broadly decreases in rocks with equivalent $^{143}Nd/^{144}Nd$ values. The East Transylvanian Basin alkali basalts (Downes *et al.*, 1995*b*) have similar $^{143}Nd/^{144}Nd$ to the low-K Călimani volcanics but lower $^{87}Sr/^{86}Sr$ at a given $^{143}Nd/^{144}Nd$. The back-arc calc-alkaline rocks from Rupea and La Gruiu Fintina have identical Sr–Nd isotope characteristics to the more enriched East Transylvanian Basin alkaline magmas (Fig. 5).

Pb isotopes (Fig. 6) exhibit more limited variation and only minor differences are observed between the different groups. $^{207}Pb/^{204}Pb$ and $^{208}Pb/^{204}Pb$ are enriched above the Northern Hemisphere Reference Line (NHRL: Hart, 1984; Fig. 6a). CGHA data plot close to (but at slightly lower $^{206}Pb/^{204}Pb$) data for the Western Carpathian (Salters *et al.*, 1988) and

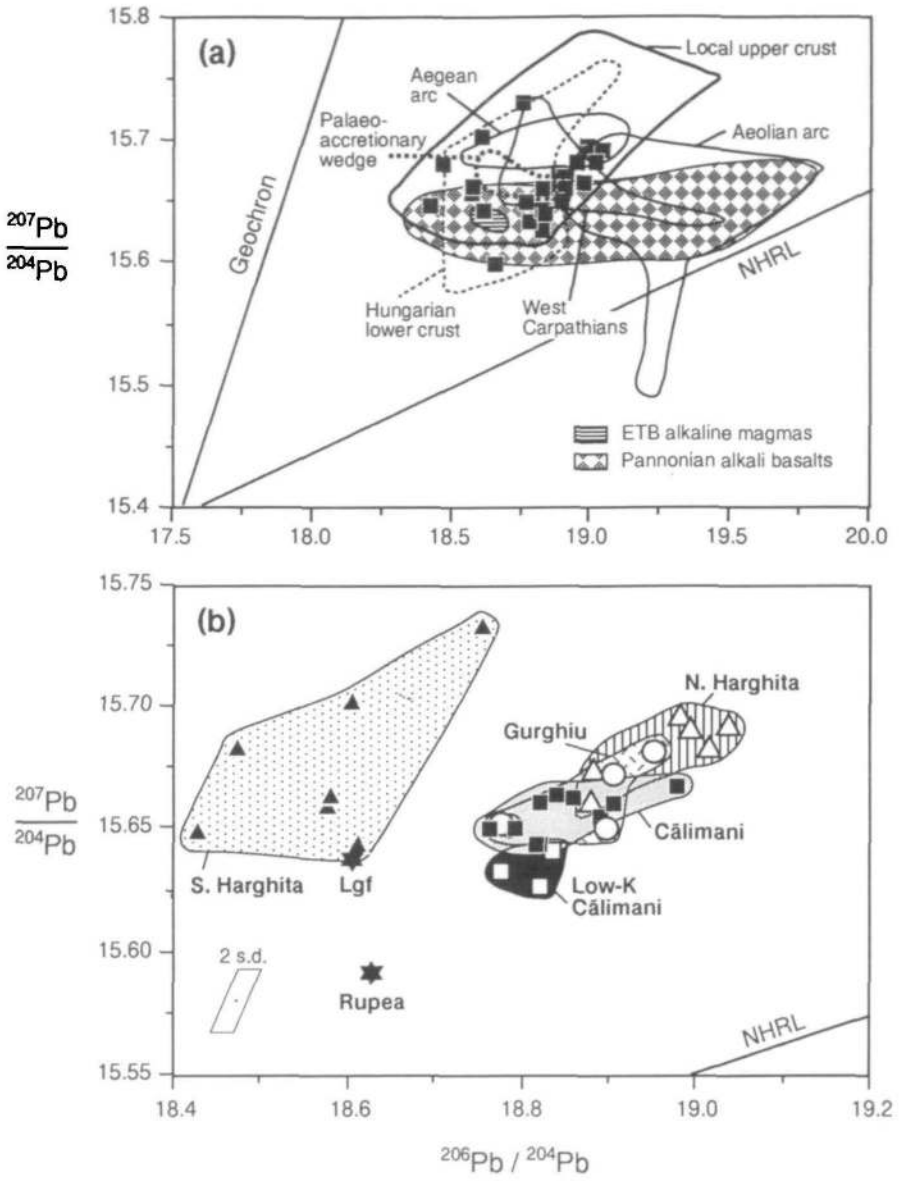

Fig. 6. Pb isotope systematics for selected CGHA volcanic and crustal samples. Symbols as in Fig. 2. (a) Comparison with other arc volcanics and mantle reservoirs in the Carpatho-Pannonian area. Data sources are as in Fig. 5 with the addition of: Hungarian lower crust—Kempton *et al.* (1993); Aegean arc—Pe-Piper (1994). The local upper-crustal signature covers the range of variation in the volcanics. (b) Variations within the groups are small and cluster close together, with the exception of the Southern Harghita group.

Aegean arcs (Pe-Piper, 1994), but do not approach the higher $^{206}Pb/^{204}Pb$ values found in the Aeolian arc (Ellam *et al.*, 1988). Eastern Transylvanian Basin alkali basalts have similar values to the lowest $^{206}Pb/^{204}Pb$ CGHA samples (Downes *et al.*, 1995*b*).

The strong enrichment trends for Sr and Nd isotopes within each group are accompanied by only small variations in Pb isotope ratios (Fig. 6b). Low-K Călimani rocks have Pb isotopic compositions closest to the NHRL ($\Delta^{207}Pb = 10–11$; $\Delta^{208}Pb = 35–41$) whereas the Călimani, Gurghiu and Northern Harghita groups plot very close together at higher $^{207}Pb/^{204}Pb$ and $^{208}Pb/^{204}Pb$ ratios (Fig. 6b). The Călimani group does not extend to as high $^{207}Pb/^{204}Pb$ and $^{208}Pb/^{204}Pb$ at an equivalent $^{206}Pb/^{204}Pb$ as the Gurghiu and Northern Harghita groups, but differences are close to analytical error. Southern Harghita magmas have lower $^{206}Pb/^{204}Pb$ (18·43–18·75) than those from the other groups, with the La Gruiu Fintina back-arc basalt plotting close to the most primitive sample. The Rupea basaltic andesite has lower $^{207}Pb/^{204}Pb$ and $^{208}Pb/^{204}Pb$ than

the CGHA samples and lies below the field for East Transylvanian Basin alkali basalts (Fig. 6a).

The local East Carpathian upper crust (Table 3, Figs 5 and 6) has highly enriched and variable isotopic compositions typical of old metasedimentary material and granitoids ($^{87}Sr/^{86}Sr = 0{\cdot}70936$–$0{\cdot}73619$; $^{143}Nd/^{144}Nd = 0{\cdot}512346$–$0{\cdot}511963$; $\Delta^{208}Pb = 37$–95). The abundant schists tend to have the highest $^{87}Sr/^{86}Sr$ ratios. The Pb isotopic composition of the local upper crust completely overlaps the Pb data field for the CGHA volcanic rocks. $^{87}Sr/^{86}Sr$ values of East Carpathian palaeo-accretionary wedge flysch sediments are fairly low ($0{\cdot}70780$–$0{\cdot}71702$) compared with the upper-crustal samples but their $^{143}Nd/^{144}Nd$ is similar ($0{\cdot}5012255$–$0{\cdot}512126$). Pb isotope ratios in the flysch samples ($\Delta^{208}Pb = 26$–68) are similar to those in present-day sediments from the Black Sea basin (Cooper *et al.*, 1974) and lie between the data fields of the Southern Harghita and Călimani groups. An Oligocene flysch sample has slightly higher $^{206}Pb/^{204}Pb$ than the Cretaceous flysch samples.

Laser fluorination oxygen isotope data

$\delta^{18}O$ values have been determined for clinopyroxene, amphibole and orthopyroxene mineral separates (Table 3), which are abundant, fresh phenocryst phases in most lithologies. Additional measurements were made on biotite, plagioclase, olivine and garnet where fresh pyroxene or amphibole was scarce or not available. Oxygen isotopes are fractionated between different mineral phases (Friedman & O'Neil, 1977) but the degree of fractionation between amphibole, pyroxene and biotite is small ($<0{\cdot}3$‰; Taylor & Sheppard, 1986) and within analytical error in most cases within this study. Data used in all figures and modelling are for pyroxene, amphibole or biotite (to remove any large-scale fractionation effects) and will be referred to as $\delta^{18}O^*$. Fractionation between these phases and basaltic magma is about $-0{\cdot}4$‰ (Taylor & Sheppard, 1986) and after extensive fractional crystallization of a typical calc-alkaline magma both the magmatic $\delta^{18}O$ value and the isotopic fractionation factor increase. We prefer to use $\delta^{18}O^*$ data for comparative purposes as they probably behave in a constant manner with fractionation, rather than make a double correction to the data.

$\delta^{18}O^*$ results for mineral phases from the CGHA cover a wide range ($5{\cdot}1$–$8{\cdot}7$‰) and are similar to $\delta^{18}O_{WR}$ values for typical island arc and continental margin arc volcanic rocks (Hoefs, 1987; Harmon & Hoefs, 1995). Variations are seen in mineral $\delta^{18}O^*$ values between lavas from different groups. The Călimani group covers a wide range in $\delta^{18}O^*$ data,

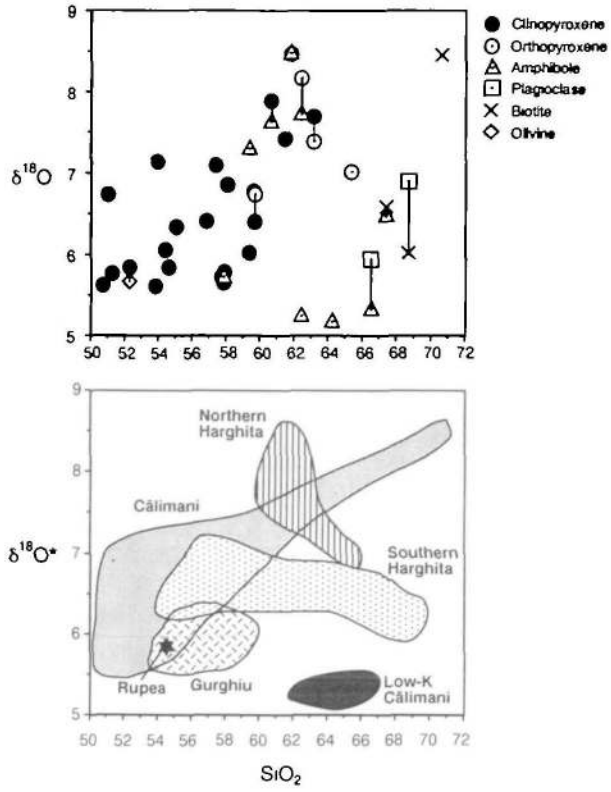

Fig. 7. SiO_2 vs $\delta^{18}O$ diagram for mineral separates from the CGHA. Mineral phases from the same rock are indicated by tie lines. The lower diagram shows data for pyroxene, amphibole and biotite only ($\delta^{18}O^*$) from each of the evolutionary groups.

with samples high in $\delta^{18}O^*$ being generally more evolved (Fig. 7) and enriched in radiogenic isotopes (Fig. 8). Northern Harghita samples contain mineral phases with exclusively high $\delta^{18}O^*$ ($>7{\cdot}0$‰) corresponding to high bulk-rock SiO_2 contents and enriched Sr isotope ratios. In contrast, Gurghiu and Southern Harghita rocks contain minerals with lower $\delta^{18}O^*$ ($<7{\cdot}2$‰) and display high $^{87}Sr/^{86}Sr$ and low $^{143}Nd/^{144}Nd$.

DISCUSSION

Fractional crystallization accounts for the bulk of the major and trace element variation in the CGHA (Mason *et al.*, 1995). The effects of this dominant petrogenetic process can be filtered by focusing on incompatible element ratios and isotopic compositions. The most critical problem to address in the CGHA is the origin of the large isotopic variation within each magma series (Figs 5–8). Highly enriched isotopic compositions ($\delta^{18}O^* = 5{\cdot}1$–$8{\cdot}7$‰; $^{87}Sr/^{86}Sr = 0{\cdot}70409$–$0{\cdot}71019$; $^{143}Nd/^{144}Nd = 0{\cdot}512902$–$0{\cdot}512391$; $^{206}Pb/^{204}Pb = 18{\cdot}43$–$19{\cdot}04$) may reflect either assimilation of continental crust or enrichment of the mantle source by sediment subduction. The

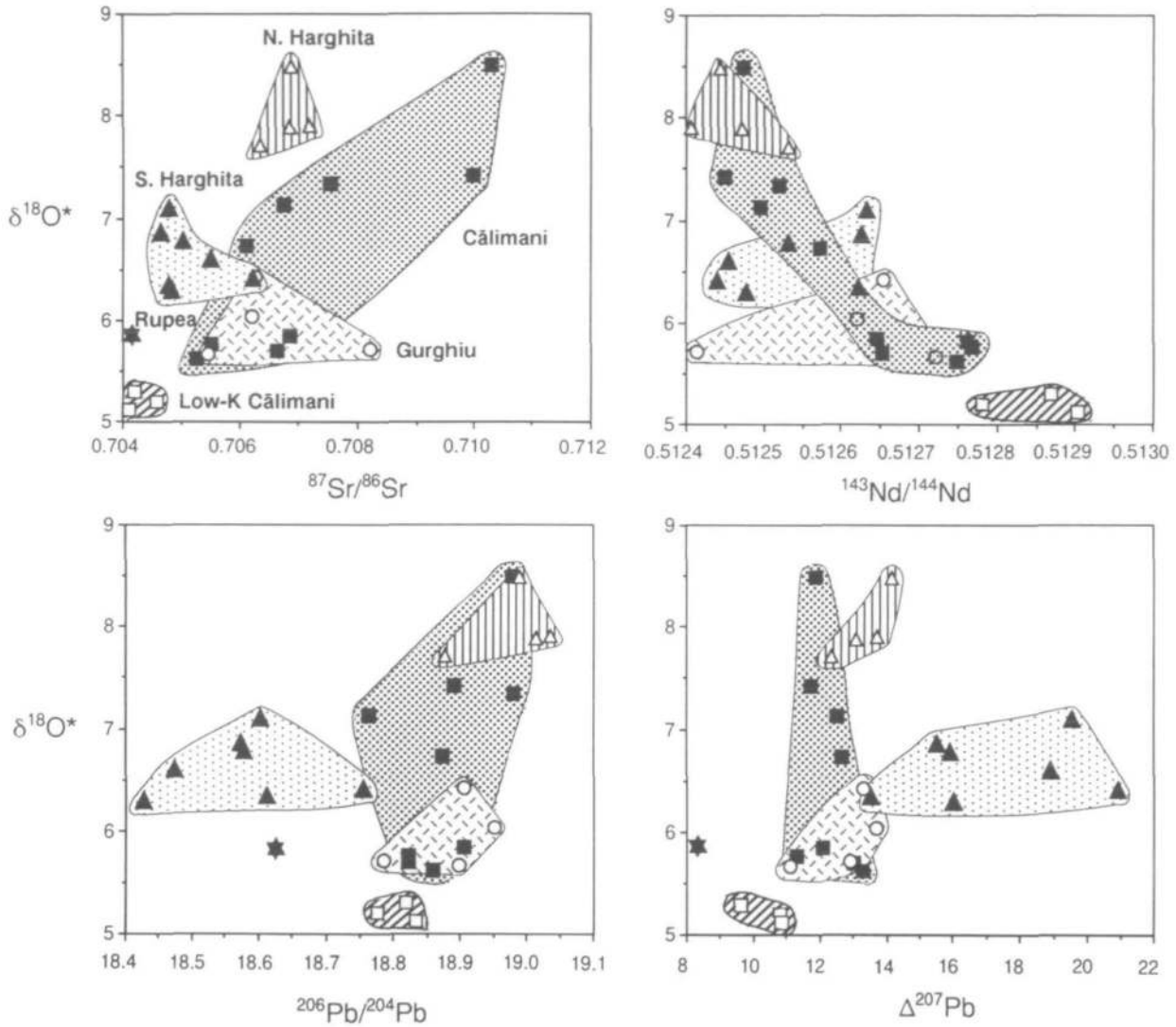

Fig. 8. $\delta^{18}O^*$ vs Sr, Nd and Pb isotopes for CGHA magmas. Symbols are as in Fig. 2.

following discussion initially focuses on the balance of evidence in favour of crustal assimilation or source enrichment. Crustal contamination effects are then quantified and removed before an attempt is made to characterize the mantle source.

Coupled variations between radiogenic and O isotopes have frequently been used to argue for or against crustal assimilation (e.g. James, 1981). In the CGHA, correlations are seen between mineral separate $\delta^{18}O^*$ and whole-rock $^{87}Sr/^{86}Sr$ and $^{143}Nd/^{144}Nd$ (Figs 8 and 9), with several magmas having both high $\delta^{18}O^*$ and low $^{143}Nd/^{144}Nd$. Local metamorphic basement has moderate to high $\delta^{18}O_{WR}$ (13·1–17·9‰, Table 3) and assimilation of this crust could produce the most isotopically enriched Călimani and Northern Harghita magmas (Fig. 9a). $\delta^{18}O_{WR}$ is used for crustal material (as opposed to $\delta^{18}O^*$), as crust is considered to be thoroughly digested during assimilation (e.g. Watson, 1982). Lower crust can frequently have low $\delta^{18}O_{WR}$ (Fowler & Harmon, 1990) and so magmas with lower $\delta^{18}O^*$ (6–7‰) may also have undergone crustal contamination (dotted assimilation trajectory in Fig. 9a). Crustal assimilation was therefore a viable process to produce the enriched radiogenic isotopic signatures in most magmas.

However, isotopic mixing lines (Fig. 9) are dependent upon the composition of the two end-members and crustal contamination may not be the only process which could produce the enriched magmatic isotopic characteristics. The interpretation of Nd–O mixing lines in Fig. 9 is governed by the Nd

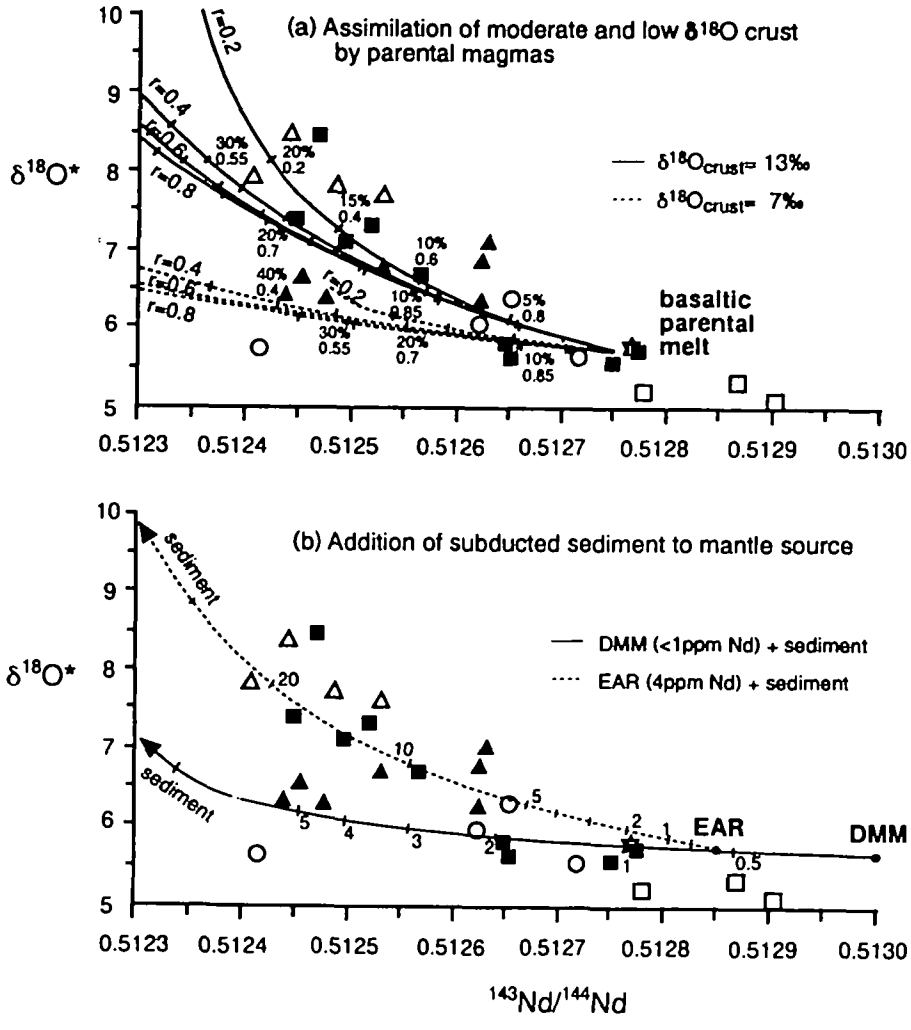

Fig. 9. Crustal assimilation and source bulk mixing models to explain Nd and O isotope variations in CGHA magmas. (a) AFC modelling for mixing between a hypothetical parental magma and local crust of variable $\delta^{18}O_{WR}$. Variations in r (degree of assimilation/degree of fractionation) are shown with tick marks for every 5% of crust consumed. Values for the amount of crust consumed and the amount of melt remaining (F) are shown for the case where $r = 0{\cdot}4$ and also for the case of $r = 0{\cdot}2$ for the high $\delta^{18}O_{WR}$ assimilant. D_{Nd} is assumed to be 0·3 in all calculations. (b) Bulk mixing calculations for addition of average palaeo-accretionary wedge sediment to a depleted MORB-source mantle and an enriched EAR mantle.

contents of the mantle source and the contaminant, the latter also having variable $\delta^{18}O_{WR}$. Bulk mixing models which approximately represent the effects of adding subducted sediment into the mantle are shown in Fig. 9b. Mixing between sediment and depleted mantle cannot generate the entire range of magmas even when varying the sediment $\delta^{18}O_{WR}$ value up to 22‰ (a probable maximum for sedimentary rocks), but mixing lines can explain the variation when adding subducted sediment to an enriched mantle source with a higher Nd content (~4 p.p.m. Nd, Fig. 9b, Table 4). However, it seems unlikely that a mantle source with such high Nd could generate the Călimani and Gurghiu basalts which have 12–15 p.p.m. Nd. Such basalts are themselves the product of substantial fractional crystallization which increased the Nd content from that of the parental magma. The maximum percentage of melting in an arc environment is unlikely to be >20%, which would generate a magma with ~14 p.p.m. Nd from an enriched peridotite source (4 p.p.m. Nd) and ~3 p.p.m. from a depleted peridotite source (<1 p.p.m. Nd). In addition, unrealistically large amounts of sediment (>10%) would be required by the mixing models to explain the isotopic variation within the enriched magmas. Thus, assimilation is the most likely process which could produce the more isotopically enriched magmas ($^{143}Nd/^{144}Nd < 0{\cdot}5127$, $\delta^{18}O^* > 7‰$).

Pb isotopes do not vary significantly with $\delta^{18}O^*$

Table 4: Compositions of parental and mantle end-members used in AFC and bulk mixing modelling

Isotopic reservoir	Călimani parental magmas		Gurghiu parental magma (GPM)	N. Harghita parental magma (NHPM)	S. Harghita parental magma (SHPM)	Depleted asthenospheric source (DMM)	Enriched asthenospheric source (EAR)
	C65	C4					
$^{87}Sr/^{86}Sr$	0·7053	0·7055	0·70409	0·70409	0·7047	0·7031	0·7037
$^{143}Nd/^{144}Nd$	0·51275	0·51278	0·512902	0·512902	0·51263	0·5130	0·51285
$^{206}Pb/^{204}Pb$	18·86	18·82	18·90	18·88	18·61	18·5	19·7
$^{207}Pb/^{204}Pb$	15·67	15·64	15·65	15·66	15·64	15·5	15·7
$^{208}Pb/^{204}Pb$	38·94	38·82	39·05	38·97	38·58	38·2	39·6
$\delta^{18}O^*$	5·7	5·7	5·7	5·7	5·7	5·7	5·7
Sr p.p.m.	320	295	300	300	950	9	66
Nd p.p.m.	16	12	14	14	17	0·73	4
Pb p.p.m.	4·8	4·8	5	5	23	0·03	0·3

Trace element concentrations for depleted and enriched asthenosphere are taken from Sun & McDonough (1989) assuming 10% melting. Isotope ratios for DMM and EAR are calculated from the composition of East Transylvanian Basin alkali basalts (Downes *et al.*, 1995*b*) and Pannonian Basin alkali basalts (Embey-Isztin *et al.*, 1993).

(e.g. Fig. 8). In the Călimani group $\delta^{18}O^*$ varies over a wide range whereas $^{206}Pb/^{204}Pb$ and $\Delta^{207}Pb$ are rather uniform. The Gurghiu and Northern Harghita groups appear to lie along the same trend as the Călimani samples. The isotopic variation could be produced by crustal assimilation from one of two initial parental magma compositions. The parental melt could have had: (1) low $\Delta^{207}Pb$ with very low $\delta^{18}O^*$ ($\sim$5·0‰), as a steep mixing trajectory would produce little Pb isotopic variation in the contaminated magmas; or (2) low $\delta^{18}O^*$ ($\sim$5·7‰) with similar $\Delta^{207}Pb$ to the contaminant. Parental basalts from Călimani have $\delta^{18}O^*$ of $\sim$5·7‰, which suggests that the latter case is more likely, i.e. parental magmas and contaminant had similar Pb isotopic signatures. The mantle source is also unlikely to have $\delta^{18}O^*$ below 5·6‰ (Mattey *et al.*, 1994). In contrast, the Southern Harghita magmas display minor variation in $\delta^{18}O^*$ with large shifts in $^{206}Pb/^{204}Pb$ and $\Delta^{207}Pb$ (Fig. 8). Contamination with crust with similar $\delta^{18}O$ to the parental magmas but radically different $\Delta^{207}Pb$ could explain the variation. However, this is unlikely as Pb/O ratios are generally high in the crust and consequently mixing curves involving expected mantle and crustal end-members would lead to homogeneous Pb isotope ratios in the magmas, which are not seen. Thus, it is likely that Pb isotopes were significantly modified from depleted mantle values before large-scale upper-crustal assimilation in all parts of the arc. This may have occurred through either lower-crustal assimilation or source enrichment by subducted sediment.

Mechanism of crustal assimilation

Interaction with the continental lithosphere was probably extensive, as magmas traversed 30–40 km of the East Carpathian crust and/or palaeo-accretionary wedge sediments to reach the surface. During ascent, crystallization, fractionation and mixing probably occurred. Isotopic and trace element modification is likely to have taken place during residence in the crust. The sampled upper crust is heterogeneous (Tables 2 and 3; Figs 4–6) but the composition of the lower crust in Romania is poorly understood. The most closely related lower-crustal rocks which have been investigated are those from the Western Pannonian Basin (Kempton *et al.*, 1993), but these are part of the separate Alcapa microplate (Csontos *et al.*, 1992) where the tectonic and magmatic history may have been significantly different. Therefore, although we will investigate the interaction between magma and upper crust, lower-crustal contamination may also have occurred but is more difficult to constrain.

Correlations between radiogenic isotopes and fractionation indices (e.g. SiO_2, MgO) have often been used as evidence for assimilation during fractionation (AFC). The fractionating mineral assemblage in common calc-alkaline magmas (e.g.

plagioclase, pyroxenes) would cause an increase in SiO_2 and a decrease in MgO during fractionation. Viewed as a whole, the CGHA data do not show clear AFC correlations and even within the identified spatial and temporal groups only weak trends are present (Fig. 10). A positive correlation occurs within the Călimani group for $^{87}Sr/^{86}Sr$ vs SiO_2 and a slight negative $^{143}Nd/^{144}Nd$ vs SiO_2 trend is observed. The low-K Călimani group shows no isotopic variation with fractionation and isotope vs fractionation index variations are also absent for the Gurghiu and Northern Harghita groups. For Northern Harghita lavas the trends are scattered, with dacitic rocks being some of the least isotopically enriched. $\delta^{18}O^*$ is high in all Northern Harghita samples but is higher in andesites than in dacites. If the dacites are excluded from this series, then a simple AFC trend could be described for the group. Clearly, crustal contamination processes in the CGHA were more complex than the simple AFC model.

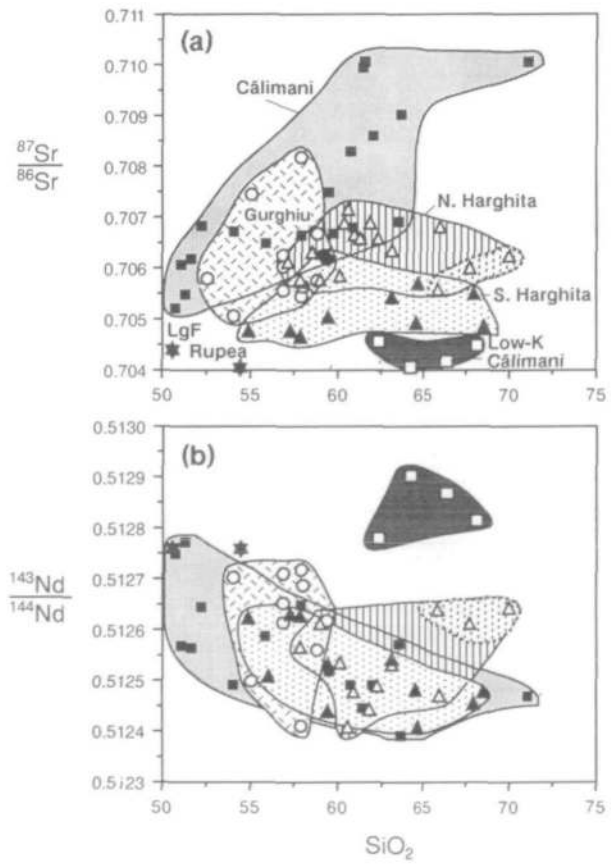

Fig. 10. Variations in Sr and Nd isotope ratios during fractional crystallization. Symbols as in Fig. 2. (a) SiO_2 vs $^{87}Sr/^{86}Sr$; (b) SiO_2 vs $^{143}Nd/^{144}Nd$. The dashed part of the Northern Harghita field represents a group of more evolved magmas with unusually depleted isotopic signatures when compared with the remainder of the group.

Differences in the isotopic signatures of the lavas might have been produced by longer residence times in thicker crust. Crustal thicknesses increase from 30 km in most of the CGHA, to 40 km in the Southern Harghita Mountains (Stănică *et al.*, 1990) and in the eastern part of the Călimani Mountains (Socolescu *et al.*, 1964; Lillie *et al.*, 1994, and references therein). At a constant $^{143}Nd/^{144}Nd$, the Călimani group have higher $^{87}Sr/^{86}Sr$, whereas the Southern Harghita group have lower $^{87}Sr/^{86}Sr$, compared with the groups erupted through the thinner crust. Significantly, $^{143}Nd/^{144}Nd$ reaches similar enriched values in both the thinner and the thicker zones. Thus, the change in the isotopic mixing trends is not directly related to the difference in crustal thickness and a more profitable argument would be to consider the possibility of different contaminants or contamination processes in different parts of the arc.

Within individual volcanic centres, the oldest lava flows and intrusions are commonly the most evolved and isotopically enriched. The few basic CGHA magmas with $^{143}Nd/^{144}Nd > 0{\cdot}5127$ all occur in large, long-lived eruptive centres. In the Călimani area the oldest flow (C16) is also the most evolved and has the highest $^{87}Sr/^{86}Sr$ and $\delta^{18}O^*$ of any magma in the CGHA. Such correlations between isotope geochemistry and field relationships suggest a simple evolution of magmatic pathways through the crust, whereby more mantle-derived magmas were only able to reach the surface through established channels and conduits. The juvenile nature of the CGHA and the rapid migration of the focus of magmatic activity through time along the strike of the arc probably contributed to the highly contaminated nature of CGHA magmas. The absence of dominant AFC as a contamination mechanism (except in the most established magmatic centre of Călimani) may also be related to the constant migration of magmas into new areas of crust.

The lack of basic and isotopically depleted magmas which reached the surface may also suggest that a zone of mixing, assimilation, storage and homogenization (MASH; Hildreth & Moorbath, 1988) operated at lower-crustal depths in the CGHA. The incorporation of crust would lead to enriched baseline isotopic characteristics in magmas, which may have been further fractionated and contaminated at shallower crustal depths through AFC. It is difficult to constrain lower-crustal contamination, owing to a lack of knowledge concerning the composition of the deep crust beneath the

CGHA. However, it is very likely that MASH was operating and differences in the isotopic characteristics of parental magmas in different parts of the arc may be a feature of MASH processes.

Quantitative AFC modelling

From the combined isotopic and chemical evidence discussed above, it appears that upper- and possibly lower-crustal assimilation were important petrogenetic processes during magma genesis in the CGHA. Although contamination probably did not follow a simple model throughout the arc, AFC modelling (DePaolo, 1981; Aitchenson & Forrest, 1994) is still the best method with which to quantify upper-crustal assimilation and to constrain the crustal contaminants. Isotopic and trace element data (Tables 2 and 3) for local crustal lithologies constrain our estimations of the enriched end-members in contamination models. The sampled upper-crustal material probably represents the range of contaminants involved. Schists are used in the modelling as these have low melting points, contain significant Sr, Nd and Pb abundances and are a major component of the crust. They are also frequently seen as crustal xenoliths in lava flows.

The least isotopically enriched and most basic magmas have been identified for each group so as to assess subsequent crustal assimilation. These generally have low mineral $\delta^{18}O^*$ ($\sim$5·7‰) but also have low MgO (<6%), low Ni (<63 p.p.m.) and low Cr (<173 p.p.m). Olivine and clinopyroxene fractionation affected the chemistry of these magmas before eruption. CGHA basic rocks have enriched $^{87}Sr/^{86}Sr$ (0·70525–0·70820) and low $^{143}Nd/^{144}Nd$ (0·512775–0·512413) at $\delta^{18}O^*$ values typical of mantle clinopyroxene (5·7‰; Mattey *et al.*, 1994). These characteristics, coupled with high K/Nb and low Ce/Pb ratios, either may have been derived from a subduction-modified mantle source or may reflect assimilation of low $\delta^{18}O_{WR}$ lower crust.

Basalts C65 and C4 are used as parental compositions for the Călimani group. These are not the most isotopically depleted magmas from the area but are related by fractionation to other more evolved Călimani magmas. Parental compositions for the Gurghiu and Northern Harghita groups have somewhat lower $^{143}Nd/^{144}Nd$ ratios. The Southern Harghita parental magma appears to have lower $^{87}Sr/^{86}Sr$ and a much higher Sr content.

AFC curves calculated using estimated parental magmas with schists as contaminants can explain the Sr, Nd, Pb and O isotope variation. Modelling is most tightly constrained using Nd and O isotopes (Fig. 9). The bulk oxygen content of the primitive and enriched end-members is identical, Nd isotopes are not affected by alteration and bulk distribution coefficients can be well constrained. Furthermore, the $^{143}Nd/^{144}Nd$ of the local upper crust is constrained to be $\sim$0·5122 (Fig. 5, Table 3). The greatest unknown is the $\delta^{18}O_{WR}$ of the crust, which may vary considerably. Figure 9a shows two models for assimilation of moderate (13‰) and low (7‰) $\delta^{18}O_{WR}$ crust. A hypothetical parental magma with the composition of basalt C65 from Călimani is used here with schist CB6 as the contaminant. Up to 25% crust is required with varying amounts of fractional crystallization (F). The closeness of the models to reality varies depending on the ratio of mass assimilant/mass crystallization (r) which is taken. D_{Nd} is assumed to be 0·3, based upon average distribution coefficients for andesitic rocks, but may vary to some extent in evolved magmas. It is significant that by varying r, the range in the data cannot be produced by a single contaminant and thus assimilation of more than one type of crust is required to explain the trends. One sample from the Gurghiu group (G32) has low $^{143}Nd/^{144}Nd$ and low $\delta^{18}O^*$, which might suggest the inheritance of low $^{143}Nd/^{144}Nd$ from the mantle source. However, this sample contains quartzitic xenoliths and hence the low $^{143}Nd/^{144}Nd$ is more likely to be the result of contamination by low $\delta^{18}O_{WR}$ crust.

Sr and Nd isotope diagrams emphasize the differences in contaminants and parental magmas along the arc (Fig. 11). The alignment of lavas from different geographical areas along different mixing trends is distinct. The Călimani and Gurghiu groups appear to diverge from a common primitive end-member close to the values of the low-K Călimani dacite group. The observed heterogeneity in upper-crustal $^{87}Sr/^{86}Sr$ (Table 3) may explain the wide variation in isotopic compositions in the Călimani, Gurghiu and Northern Harghita groups, at the enriched ends of these arrays. A similar model may apply to the Southern Harghita and back-arc magmas but involving a parental magma of similar $^{87}Sr/^{86}Sr$, but slightly lower $^{143}Nd/^{144}Nd$.

An important variable in the Sr isotope modelling is the Sr content of the initial magma (e.g. Sr = 300–420 p.p.m. for basaltic rocks in the Călimani group). This can have a significant effect on contamination models and precludes the exact identification of the crustal contaminant involved. However, more than one contaminant is required to explain the isotopic variation in different parts of the arc. Both metamorphic basement rocks and flysch sediments may have been assimilated in the Călimani area (Fig. 11a). It is difficult to generate the magmas with

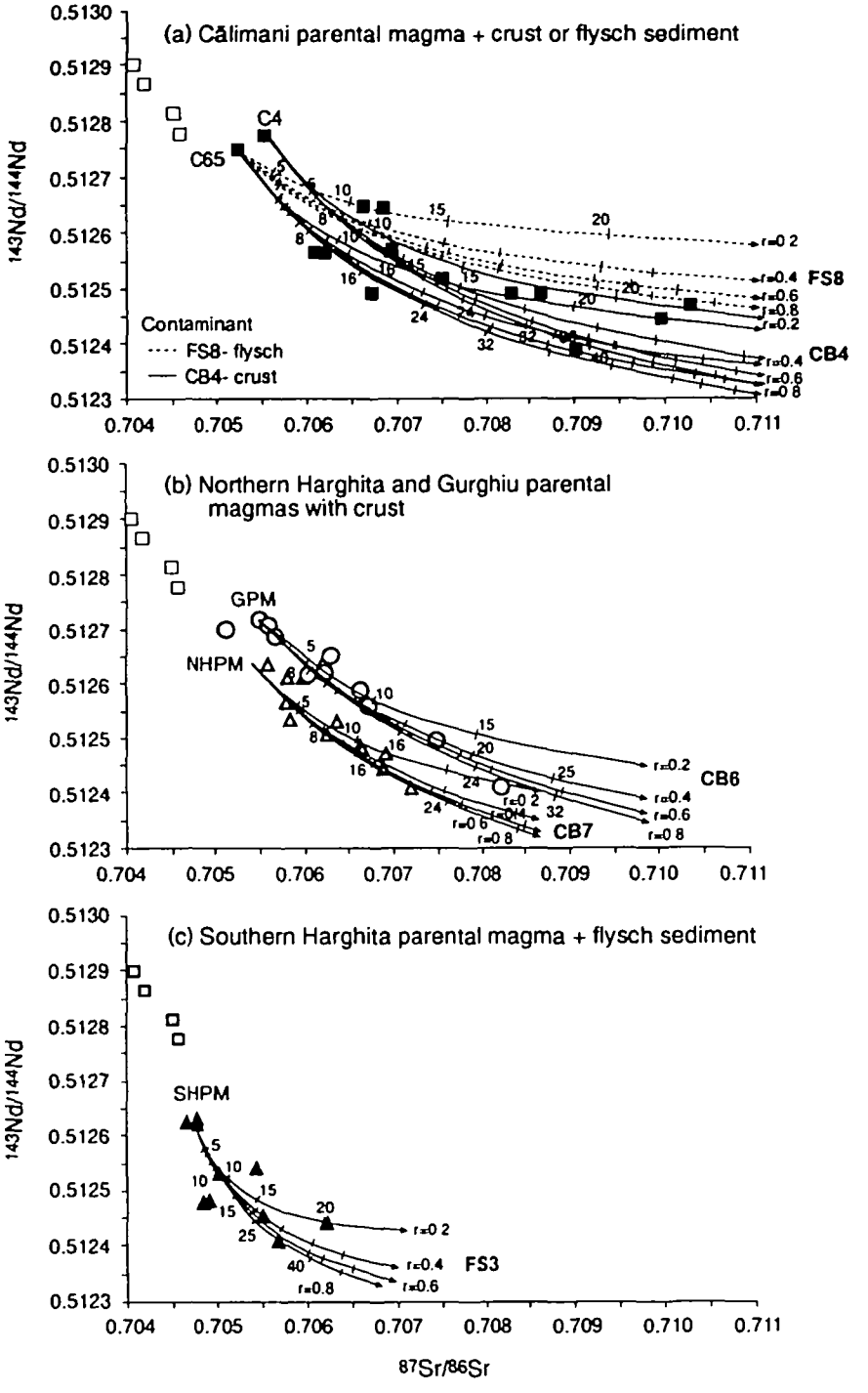

Fig. 11. AFC trajectories using Sr and Nd isotopes for assimilation of local crust by parental magmas in the CGHA. (a) Both metamorphic upper crust and flysch sediment could explain enriched isotopic compositions in the Călimani area. Tick marks show the amount of crust consumed (%). (b) Slightly different parental magmas and contaminants could explain differences in Sr and Nd isotopes between the Gurghiu and Northern Harghita areas. GPM, Gurghiu parental magma; NHPM, Northern Harghita parental magma (compositions are in Table 4). Tick marks show the amount of crust consumed (%). (c) Calculated mixing trajectories for assimilation of palaeo-accretionary wedge sediments in the Southern Harghita area. Upper-crustal AFC between a parental basaltic magma SHPM (Table 4) and adjacent shales from the accretionary wedge (Tables 2 and 3).

$^{87}Sr/^{86}Sr = 0{\cdot}7065$ and $^{143}Nd/^{144}Nd = 0{\cdot}51265$ with the sampled metamorphic basement as a sole contaminant. Flysch may also have been incorporated and an AFC model is shown in Fig. 11a using Oligocene sediments from the southern Flysch belt which are probably similar to those in the Călimani area. Between 5 and 35% assimilation of crustal material is required to explain the isotopic variation.

Crustal schists are the most likely contaminants in the Gurghiu and Northern Harghita areas (Fig. 1), and modelling using these compositions explains the isotopic enrichment well. The data for these magma series are rather tightly defined along two simple AFC trajectories (Fig. 11b), suggesting slightly different crustal compositions in each area.

In the Southern Harghita area, AFC calculations suggest the assimilation of 10–35% flysch sediment by parental magma SHPM (Fig. 11c, Table 4). However, $\delta^{18}O^*$ is fairly low in all Southern Harghita magmas (6·3–7·1‰, Figs 7 and 8), suggesting that such extensive crustal assimilation with high $\delta^{18}O_{WR}$ flysch is not feasible. Contamination with low $\delta^{18}O_{WR}$ crust could be one explanation for this variation but flysch sediment is unlikely to be low in $\delta^{18}O_{WR}$ at either upper- or lower-crustal depths. The evidence for assimilation is weak but values of $\delta^{18}O^* \geqslant 7‰$ are probably too high to have been produced solely through sediment subduction into the mantle source. Some of the variation to low $^{87}Sr/^{86}Sr$ in the Southern Harghita group is probably due to the higher Sr/Nd ratio of parental magmas in this part of the chain. Samples H4 (Sr/Nd = 54·6) and H6 (Sr/Nd = 73·5) have slightly lower $^{87}Sr/^{86}Sr$ at low $^{143}Nd/^{144}Nd$ with the sample with the greater Sr/Nd ratio having the lower $^{87}Sr/^{86}Sr$. Mixing trajectories have been modified reflecting the lesser impact of the contaminant on $^{87}Sr/^{86}Sr$ in a magma with a greater Sr content.

In summary, much of the Sr, Nd and O isotope variations can be explained by crustal assimilation between the least isotopically enriched parental magmas and schists from the local upper crust or terrigenous sediments from the palaeo-accretionary wedge. Variations in Sr and Nd isotope correlations correspond to variations in parental magmas and variations in basement lithologies from schist to flysch sediment (Fig. 11).

Identification of mantle-derived magmas

The characterization of primary mantle-derived magmas is contentious for the CGHA, as in many continental margin arcs. Basaltic magmas in equilibrium with a typical depleted mantle source would be expected to have high Ni concentrations, MgO >8%, $\delta^{18}O^* \sim 5{\cdot}7$ and high Ce/Pb (>12). Parental magmas from the CGHA are fractionated and small amounts of contamination, particularly at lower-crustal depths, cannot be ruled out owing to their elevated $\delta^{18}O^*$ values. It is not clear whether their radiogenic isotopic characteristics have been derived from the mantle source or are due to assimilation at the base of the crust. Other local mantle reservoirs must be considered, to aid the characterization of primary arc magmas.

Asthenosphere-derived alkali basaltic volcanism occurred contemporaneously with calc-alkaline activity at the southern end of the CGHA (Downes *et al.*, 1995*b*). Enriched mantle signatures [European Asthenospheric Reservoir (EAR); Cebriá & Wilson, 1995] which lie between depleted and HIMU compositions have been observed in parts of the European asthenosphere (Wilson & Downes, 1991; Hoernle *et al.*, 1995). Pb isotopes in the East Transylvanian Basin alkali basalts and in basalts across the Pannonian Basin trend away from an initial mantle of EAR composition (Embey-Isztin *et al.*, 1993; Downes *et al.*, 1995*b*). Back-arc basic calc-alkaline rocks are closely associated with the alkaline magmas (Fig. 4) and are isotopically identical to the enriched end of the alkali basalt field (Fig. 5b). Thus the back-arc rocks and the alkali basalts may have been derived from the same mantle source. Southern Harghita group lavas, in turn, trend away from the back-arc basalts on Sr, Nd and Pb isotope diagrams (Figs 5 and 6) and so the true parental magma for the Southern Harghita group may have been similar to the back-arc magmas. This primary isotopic composition is significantly more primitive than the previously proposed parental Southern Harghita arc lava (SHPM, Table 4). The mantle wedge beneath the Southern Harghita area may thus have EAR characteristics which are reflected in the alkaline and calc-alkaline magmas.

There is no reason to extrapolate an enriched EAR signature across the entire CGHA mantle wedge, the bulk of which may be depleted MORB-source mantle, as has been suggested for many arcs (e.g. White & Dupré, 1986). Pb isotope compositions (Fig. 6) for the most primitive lavas from the remainder of the CGHA are similar to those of the alkali basalts but there are differences in the Sr and Nd isotopic ratios, with the most primitive Călimani and Gurghiu calc-alkaline rocks having higher $^{87}Sr/^{86}Sr$ at a similar $^{143}Nd/^{144}Nd$ (Fig. 5). A MORB source would be more consistent with trace element levels in Călimani and Gurghiu basalts, as it would be difficult to generate basic magmas with ~3 p.p.m. Nb from an enriched mantle (EAR) source with no more than 20% partial melting.

The most isotopically primitive CGHA lavas are the low-K Călimani group, of which dacite C8 has the most depleted Sr and Nd isotopic composition ($^{87}Sr/^{86}Sr = 0{\cdot}70409$; $^{143}Nd/^{144}Nd = 0{\cdot}512902$; Figs 5 and 6). The covariation in $^{87}Sr/^{86}Sr$ vs $^{143}Nd/^{144}Nd$ within the low-K Călimani group may be due to a small amount of crustal assimilation but there is no corresponding increase in $\delta^{18}O^*$. These rocks have low incompatible element concentrations compared with other CGHA samples; this feature could be due to a lower degree of contamination within the crust. However, their Pb/Nd and Ce/Pb ratios and Pb isotope ratios are similar to other isotopically enriched samples, and this suggests either that the magmas are indeed contaminated or that the local mantle has elevated $^{207}Pb/^{204}Pb$ and low Ce/Pb. Pb isotopes appear to be decoupled from Sr and Nd isotopes but Pb is a much more sensitive indicator of contamination than other isotopes and trace elements. $\delta^{18}O^*$ for separated mafic minerals from dacite C8 range from 5·1 to 5·4‰, somewhat lower than expected values for pyroxenes in mantle-derived melts. Fractionation factors between magmas and clinopyroxene or amphibole are not well documented in evolved melt compositions; however, $\delta^{18}O_{plagioclase}$ is also low in the low-K dacites. Thus, the low $\delta^{18}O_{WR}$ probably represents an unusually low magmatic $\delta^{18}O$ and may reflect interaction with a contaminant with very low $\delta^{18}O^*$, such as hydrothermally altered crust.

The low-K Călimani dacites may have been derived from more basic magmas which existed at mantle or lower-crustal depths, before large-scale crustal assimilation, although basic rocks with the isotopic characteristics of this group have not been identified within the CGHA. Trace element abundances (e.g. low Y, low Cr) indicate extensive fractionation of mafic minerals, but extensive plagioclase fractionation is precluded by similar Sr/Nd ratios to other Călimani samples (Fig. 4). On some major element diagrams (e.g. SiO_2 vs K_2O) the low-K dacites appear to be related to other more basic Călimani andesites. However, these andesites have more enriched isotopic signatures than the low-K dacites and higher Pb, Rb and Th contents. Thus, it is unlikely that the dacites were directly related to the more basic Călimani magmas.

A basaltic magma with the same isotopic composition as the low-K Călimani dacites may be close to a primary mantle-derived magma. Sediment subduction may have increased $^{87}Sr/^{86}Sr$ and $\Delta^{207}Pb$, and decreased $^{143}Nd/^{144}Nd$ from an even more depleted mantle composition.

Evidence for sediment subduction

After subtracting the effects of crustal assimilation, enrichment of the initial mantle composition by subducted sediment may be investigated. Sediment may be introduced into the mantle source region of the magmas by addition from the subducted slab through fluid release or melting (Thirlwall, 1983; Arculus & Powell, 1986; White & Dupré, 1986). Potential sediment sources in the Carpatho-Scythian area include: (1) pelagic sediment on the subducted oceanic crust; (2) terrigenous sediment derived from the Scythian platform–Ukrainian shield area; (3) sediments eroded from the Carpathians and recycled into the fore-arc trench. Any of these sediment types could have been subducted into the mantle. Carpathian flysch sediments and present-day Black Sea sediments (Cooper *et al.*, 1974) are probably chemically and isotopically similar to subducted material (Table 4).

Sediment subduction beneath the Carpathian arc has been suggested on the basis of Pb isotope variations in the Eastern Transylvanian Basin alkali basalts (Downes *et al.*, 1995*b*). Mixing with continental material produced a strong variation within the magmas from EAR values to lower $^{206}Pb/^{204}Pb$ at a constant $^{207}Pb/^{204}Pb$. Crustal contamination was thought to be minimal because of the presence of mantle xenoliths within the alkali basalts (Downes *et al.*, 1995*b*). However, the Pb isotopic data may also be explained by the high-level assimilation of Western Pannonian Basin lower crust.

Modelling of Sr, Nd and Pb isotopes indicates that depleted MORB-source mantle could give rise to the low-K Călimani isotopic reservoir by bulk mixing with $<1\%$ subducted terrigenous sediment (Fig. 12). The exact amount of sediment added to the source cannot be quantified owing to a lack of constraints on the isotopic composition of the pristine mantle wedge.

Enriched EAR mantle could also give rise to a mafic precursor to the low-K Călimani dacites. However, much larger amounts of mixing (5–10%) would be required to produce the parental magmas of the CGHA because of the high Sr and Nd contents of the EAR mantle source. These amounts are inconsistent with the amount of sediment commonly believed to be added to a subduction zone mantle source (e.g. Whitford *et al.*, 1981; Vroon *et al.*, 1993) and the presence of a thick palaeo-accretionary wedge in the Carpathians. Thus a depleted MORB-source mantle beneath these areas is more probable.

For the Southern Harghita magmas, an enriched EAR mantle source could closely resemble the mantle end-member (Fig. 12), with models requiring

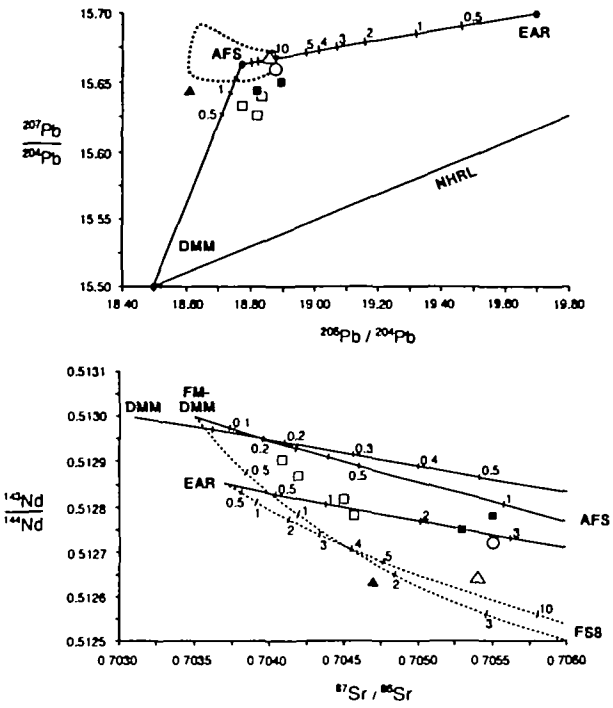

Fig. 12. Bulk mixing curves for the addition of subducted terrigenous sediment to the mantle source region. Mixing is shown between three different mantle compositions: depleted MORB-source mantle (DMM), fluid modified DMM (FM-DMM: $^{87}Sr/^{86}Sr = 0{\cdot}7035$; $^{143}Nd/^{144}Nd = 0{\cdot}5130$; Sr 20 p.p.m.; Nd 0·9 p.p.m.) and enriched European asthenosphere (EAR) (Table 4). Average flysch sediment (AFS) and Oligocene flysch (FS8) are used to represent the subducted sedimentary component. Tick marks show the percentage of sediment which should be added to the source.

the addition of a few percent sediment to produce parental calc-alkaline melts. However, the subduction of average flysch sediment cannot produce the parental melts and it is necessary to use Oligocene flysch FS8 as the subducted material. Oligocene sediments may have more closely resembled the subducted component than the Cretaceous material during the final stages of subduction in the late Miocene. Fluid-modified depleted mantle could also give rise to the lower $^{87}Sr/^{86}Sr$ seen in Southern Harghita parental magmas (Fig. 12). A greater flux of fluids from the downgoing lithospheric slab would be consistent with the high Ba/La and Sr/Nd ratios which are seen in the magmas.

In conclusion, the enriched isotopic characteristics of parental magmas can be explained by the addition of local sediment to the mantle source via subduction. However, it is not possible to distinguish this process from lower-crustal MASH or AFC, which could produce identical effects.

Summary of isotopic mixing

Figure 13 summarizes the relationship between Sr, Nd, Pb and O isotopes in CGHA magmas. Correlations between Nd and Pb isotopes show various trends along the strike of the arc. The interpretation of the trends is complex but it is possible to identify several end-members from these diagrams:

(1) A component high in ε_{Nd} from which the Călimani, Gurghiu and Northern Harghita magmas appear to be derived. This is probably similar to, or slightly enriched above an initial depleted mantle composition. The low-K Călimani group (with magma C8 as an end-member) is closely related to this primary isotopic reservoir. The Southern Harghita magmas may be related to a slightly enriched or fluid-modified mantle end-member with lower $^{206}Pb/^{204}Pb$ which was the source of the back-arc basaltic rocks (LgF).

(2) A crustal component which is high and variable in $^{206}Pb/^{204}Pb$ ($>18{\cdot}7$), has variable $\Delta^{208}Pb$ (40–80), moderate to high $^{87}Sr/^{86}Sr$ and high $\delta^{18}O_{WR}$ ($>8‰$). Two distinct mixing trends can be identified owing to variations in the chemistry and isotopic characteristics of this contaminant. The first trend is shown by all the Northern Harghita samples, most of the Gurghiu and some of the Călimani. It is probably contained in the metamorphic upper crust which underlies this region and may be close in composition to schist CB6 (Fig. 13). A second possible trend describes a mixing trajectory which passes through the data with lower $^{206}Pb/^{204}Pb$. None of the sampled crust can explain these magmas but it is likely that a crustal contaminant does exist to explain this trend which has not yet been identified. SiO_2 correlates with ε_{Nd} and $^{87}Sr/^{86}Sr$ for magmas on this trend, confirming AFC as a contamination mechanism. Most of the magmas in Călimani and some Gurghiu samples lie on this trend. This composition probably represents the bulk crust beneath the north of the CGHA where AFC was able to operate more effectively in longer-lived magmatic systems.

(3) The second crustal component is low in $^{206}Pb/^{204}Pb$ ($<18{\cdot}65$), has very high $\Delta^{208}Pb$ (>70), low $^{143}Nd/^{144}Nd$, low $^{87}Sr/^{86}Sr$, low to moderate $\delta^{18}O_{WR}$ ($\sim 6{\cdot}5‰$) and has high Sr and Pb contents. Most Southern Harghita group magmas trend towards this isotopic composition. $^{143}Nd/^{144}Nd$ and $^{206}Pb/^{204}Pb$ decrease as SiO_2 increases within the magmas, suggesting modification within the crust. The upper crust in this area is overlain by the edge of the thick palaeo-accretionary flysch wedge. Sediments from the flysch wedge could have been assimilated at upper- or lower-crustal depths owing

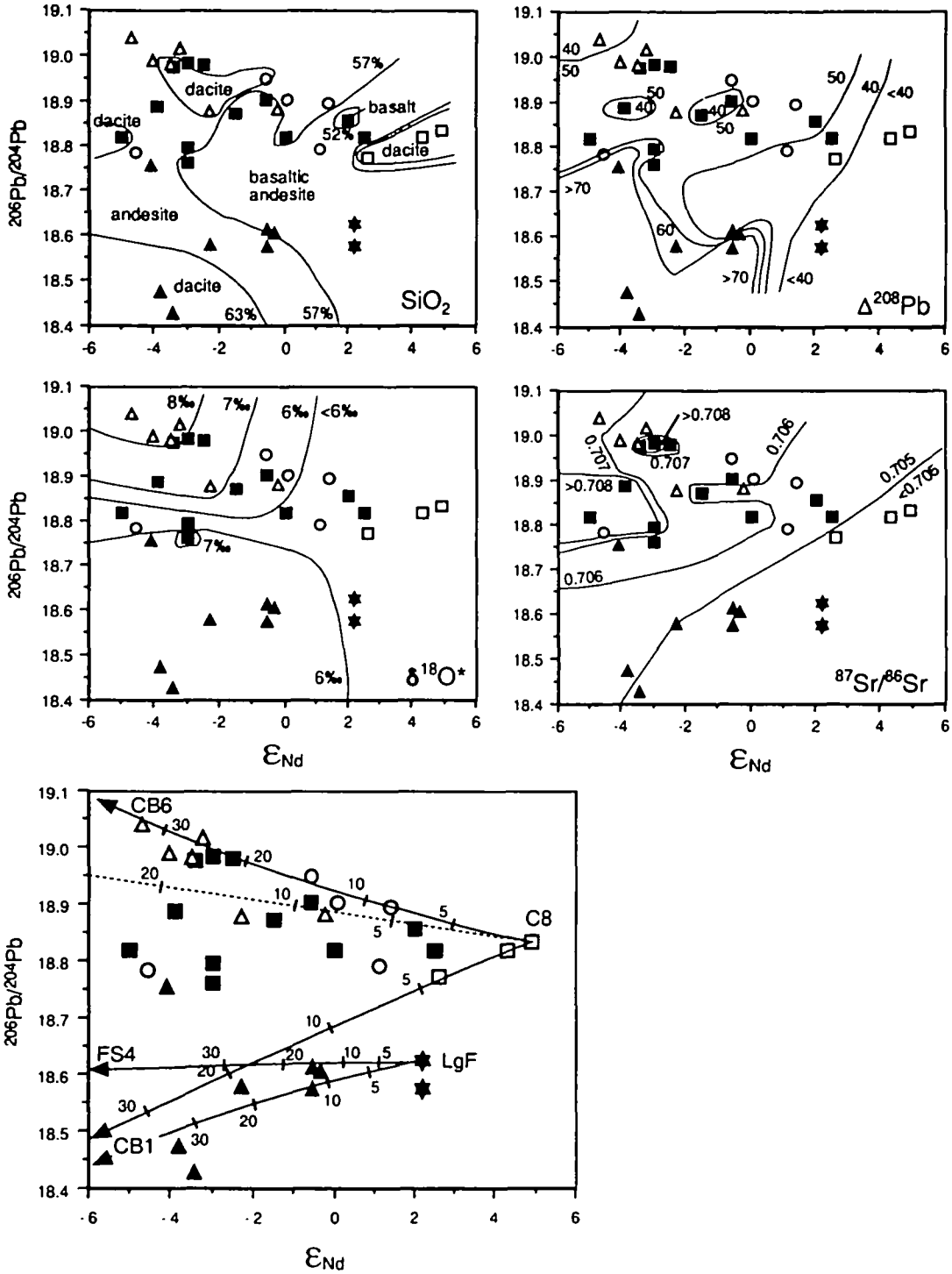

Fig. 13. Summary diagram of isotopic systematics in the CGHA. ε_{Nd} vs $^{206}Pb/^{204}Pb$ diagrams are contoured for SiO_2 concentrations, $\Delta^{208}Pb$ and $\delta^{18}O$ values, and $^{87}Sr/^{86}Sr$ ratios. AFC mixing trajectories are shown in the lower diagram for contamination of parental magmas with the composition of C8 and LgF. Crustal samples CB6 and CB1 and palaeo-accretionary wedge sediment FS4 are used as contaminants. $r = 0{\cdot}4$ in all calculations. The dotted line shows the effect of varying the Pb/Nd ratio of the assimilant. In this assimilation trajectory CB6 has a maximum possible Pb/Nd ratio of 0·1.

to the probable underthrust nature of the accretionary prism (Tomek & Hall, 1993). However, the flysch does not have as high $\Delta^{208}Pb$ as the magmas. $\delta^{18}O_{WR}$ of the flysch is likely to be high (>16‰), a feature which is not reflected in the low $\delta^{18}O^*$ of the magmas (<7‰). The assimilation of crust from the Tisza–Dacia metamorphic basement was unlikely in this area, as there is no tectonic evidence for the presence of this material at depth. This Southern Harghita crustal component has not yet been identified in the sampled palaeo-accretionary wedge or upper crust.

CONCLUDING REMARKS

The calc-alkaline volcanic rocks of the East Carpathian arc are related to a Miocene convergence and subduction event. Volcanic centres can be classified into groups of a similar age, location and internal magmatic evolution. From a new, extensive geochemical and isotopic database we conclude that fractional crystallization and crustal assimilation are dominant petrogenetic processes in the CGHA. Variations in the upper-crustal contaminant and the parental magmas along the arc could be responsible for most of the Sr, Nd, Pb and O isotope heterogeneity. Between 5 and 35% upper crust is required in AFC modelling to account for the range in observed isotope ratios.

Upper-crustal contamination has strongly masked the mantle source within this continental margin arc environment, a feature which may be common among juvenile, short-lived continental arcs. The most primitive arc magmas can be produced by adding ~0·5% subducted terrigenous sediment to a depleted MORB-source or EAR mantle. However, this process cannot be conclusively distinguished from lower-crustal MASH or AFC.

Petrogenetic processes within the five groups defined in this study can be summarized as follows:

(1) Low-K Călimani group: crustal contamination in the dacites was minor in comparison with the rest of the arc. Unseen basalts at depth, to which the dacites are related by fractionation, are postulated to form the most primitive magma for most of the CGHA.

(2) Călimani, Gurghiu and Northern Harghita groups: parental magmas are not readily identified, but the least isotopically enriched basalts or basaltic andesites can be used as a baseline magmatic composition. Magmas were strongly contaminated by local upper-crustal schists and possibly palaeo-accretionary wedge sediments in the Călimani area.

(iii) Southern Harghita group: a slightly different mantle source with lower $^{87}Sr/^{86}Sr$ and $^{206}Pb/^{204}Pb$ than the remainder of the arc was enriched in Ba and Sr. Back-arc calc-alkaline lavas most closely resemble this source. Some contamination took place in the upper crust with sediment of the palaeo-accretionary wedge, but the main crustal component has not been identified.

ACKNOWLEDGEMENTS

G. Wörner and two anonymous reviewers are thanked for constructive criticism and M. Wilson provided invaluable advice concerning an earlier version of this manuscript. Laboratory managers and staff are thanked for their help during analytical work, particularly Giz Marriner, Pieter Vroon and Gerry Ingram. P. Greenwood is thanked for carrying out whole-rock oxygen isotope analyses at the NERC Isotope Geosciences Laboratory, Keyworth, UK. This research has benefited from useful discussions with research students and staff at Royal Holloway, University of London. XRF and stable radiogenic isotope facilities at Royal Holloway are University of London Intercollegiate research services. Fieldwork was supported by the Geological Institute of Romania. P.M. acknowledges a postgraduate research studentship from NERC. H.D. is grateful for support from the Birkbeck College Research Fund and the University of London Central Research Fund.

REFERENCES

Aitcheson, S. J. & Forrest, A. H., 1994. Quantification of crustal contamination in open magmatic systems. *Journal of Petrology* **35**, 461–488.

Arculus, R. J. & Powell, R., 1986. Source component mixing in the regions of arc magma generation. *Journal of Geophysical Research* **91**(B6), 5913–5926.

Balintoni, I. & Gheuca, I., 1977. Metamorphism progresiv, metamorphism regresiv si tectonica in regiunea Zugreni-Barnar (Carpatii Orientali). *Dari de Seama ale Institutului de Géologie si Géofizica* **LXIII**, 11–38.

Balla, Z., 1987. Tertiary palaeomagnetic data for the Carpatho-Pannonian region in the light of Miocene rotation kinematics. *Tectonophysics* **139**, 67–98.

Barton, M., Salters, V. J. M. & Huijsmans, J. P. P., 1983. Sr isotope and trace element evidence for the role of continental crust in calc-alkaline volcanism on Santorini and Milos, Aegean Sea, Greece. *Earth and Planetary Science Letters* **63**, 273–291.

Bleahu, M. D., Boccaletti, M., Manetti, P. & Peltz, S., 1973. Neogene Carpathian Arc: a continental arc displaying the features of an 'island arc'. *Journal of Geophysical Research* **78**, 5025–5032.

Boccaletti, M., Manetti, P., Peccerillo, A. & Peltz, S., 1973. Young volcanism in the Călimani–Harghita Mountains (East Carpathians): evidence of a palaeoseismic zone. *Tectonophysics* **19**, 299–313.

Briqueu, L., Javoy, M., Lancelot, J. R. & Tatsumoto, M., 1986. Isotope geochemistry of recent magmatism in the Aegean arc: Sr, Nd, Hf and O isotopic ratios in the lavas of Milos and Santorini—geodynamic implications. *Earth and Planetary Science Letters* **80**, 41–54.

Burchfiel, B. C., 1976. Geology of Romania. *Geological Society of America Special Publication* **158**, 82 pp.

Cebriá, J. M. & Wilson, M., 1995. Cenozoic mafic magmatism in Western/Central Europe: a common European asthenospheric reservoir? *Terra Nova* **7**, 162.

Cooper, J. A., Dasch, E. J. & Kaye, M., 1974. Isotopic and elemental geochemistry of Black Sea sediments. In: Degens, E. T. & Ross, D. A. (eds) *The Black Sea—Geology, Chemistry and Biology. American Association of Petroleum Geologists Memoir* **20**, 554–565.

Csontos, L., Nagymarosy, A., Horváth, F. & Kovác, M., 1992. Tertiary evolution of the Intra-Carpathian area: a model. *Tectonophysics* **208**, 221–241.

Davidson, J. P., McMillan, N. J., Moorbath, S., Wörner, G., Harmon, R. S. & Lopez-Escobar, L. 1990. The Nevados de Payachata volcanic region 18°S/69°W, N. Chile II. Evidence for widespread crustal involvement in Andean magmatism. *Contributions to Mineralogy and Petrology* **105**, 412–432.

DePaolo, D. J., 1981. Trace element and isotopic effects of combined wallrock assimilation and fractional crystallisation. *Earth and Planetary Science Letters* **53**, 189–202.

Downes, H., Panto, Gy., Póka, T., Mattey, D. P. & Greenwood, P. B., 1995*a*. Calc-alkaline volcanics of the Inner Carpathian arc, Northern Hungary: new geochemical and oxygen isotope results. *Acta Vulcanologica* **7**, 29–41.

Downes, H., Seghedi, I., Szakács, A., Dobosi, G., Vaselli, O., James, D. E., Rigby, I. J., Thirlwall, M. F., Rex, D. & Pécskay, Z., 1995*b*. Petrology and geochemistry of late Tertiary/Quaternary mafic alkaline volcanism in Romania. *Lithos* **35**, 65–81.

Ellam, R. M., Menzies, M. A., Hawkesworth, C. J., Leeman, W. P., Rosi, M. & Serri, G., 1988. The transition from calc-alkaline to potassic orogenic magmatism in the Aeolian Islands, Southern Italy. *Bulletin of Volcanology* **50**, 386–398.

Embey-Isztin, A., Downes, H., James, D. E., Upton, B. G. J., Dobosi, G., Ingram, G. A., Harmon, R. S. & Scharbert, H. G., 1993. The petrogenesis of Pliocene alkaline volcanic rocks from the Pannonian Basin, Eastern Central Europe. *Journal of Petrology* **34**, 317–343.

Fowler, M. B. & Harmon, R. S., 1990. The oxygen isotope composition of lower crustal granulite xenoliths. In: Vielzeuf, D. & Vidal, Ph. (eds) *Granulites and Crustal Evolution*. Dordrecht: Kluwer Academic, pp. 493–506.

Friedman, I. & O'Neil, J. R., 1977. Compilation of stable isotope fractionation factors of geochemical interest. Data of geochemistry. *US Geological Survey Professional Paper* **440**, KK.

Gill, J. B., 1981. *Orogenic Andesites and Plate Tectonics*. New York: Springer-Verlag, 370 pp.

Harmon, R. S. & Hoefs, J., 1995. Oxygen isotope heterogeneity of the mantle deduced from a global analysis of basalts from different tectonic settings. *Contributions to Mineralogy and Petrology* **120**, 95–114.

Hart, S. R., 1984. The Dupal anomaly: a large scale isotopic anomaly in the southern hemisphere. *Nature* **309**, 753–756.

Hildreth, W. & Moorbath, S., 1988. Crustal contributions to arc magmatism in the Andes of Central Chile. *Contributions to Mineralogy and Petrology* **98**, 455–489.

Hoefs, J., 1987. *Stable Isotope Geochemistry*, 3rd edn. Berlin: Springer-Verlag.

Hoernle, K., Zhang, Y-S. & Graham, D., 1995. Seismic and geochemical evidence for large-scale mantle upwelling beneath the Eastern Atlantic and Western and Central Europe. *Nature* **374**, 34–39.

Horváth, F., 1988. Neotectonic behaviour of the Alpine–Mediterranean region. In: Royden, L. H. & Horváth, F. (eds) *The Pannonian Basin. American Association of Petroleum Geologists Memoir* **45**, 49–55.

James, D. E., 1981. The combined use of oxygen and radiogenic isotopes as indicators of crustal contamination. *Annual Review of Earth and Planetary Sciences* **9**, 311–344.

James, D. E. J., 1982. A combined O, Sr, Nd and Pb isotopic and trace element study of crustal contamination in central Andean lavas, I. Local geochemical variations. *Earth and Planetary Science Letters* **57**, 47–62.

Kempton, P. D., Downes, H. & Ionov, D. A., 1993. Deep crustal xenoliths: evidence for extreme compositional diversity in the lower crust beneath European rifts. *Terra Abstracts, Supplement 1 to Terra Nova* **5**, 427.

Leeman, W. P., 1982. Tectonic and magmatic significance of strontium isotope variations in Cenozoic volcanic rocks from the western United States. *Geological Society of America Bulletin* **93**, 487–503.

Lillie, R. J., Bielik, M., Babuska, V. & Plomerova, J., 1994. Gravity modelling of the lithosphere in the Eastern Alpine–Western Carpathian–Pannonian Basin region. *Tectonophysics* **231**, 215–235.

Mason, P. R. D., 1995. Petrogenesis of subduction-related volcanic rocks from the East Carpathians, Romania. Ph.D. Thesis, University of London, 264 pp.

Mason, P. R. D., Downes, H., Seghedi, I., Szakács, A. & Thirlwall, M., 1995. Low pressure evolution of magmas from the Călimani, Gurghiu and Harghita Mountains, East Carpathians. *Acta Vulcanologica* **7**, 43–52.

Mattey, D. & Macpherson, C., 1993. Oxygen isotope analysis of ferromagnesian minerals using the laser fluorination technique. *Chemical Geology* **105**, 305–318.

Mattey, D., Lowry, D. & Macpherson, C., 1994. Oxygen isotope composition of mantle peridotite. *Earth and Planetary Science Letters* **128**, 231–241.

Oncescu, M. C., Burlacu, V., Anghel, M. & Smalbergher, V., 1984. Three-dimensional P-wave velocity image under the Carpathian Arc. *Tectonophysics* **106**, 305–319.

Pana, D. & Erdmer, P., 1994. Alpine crustal shear zones and prealpine basement terranes in the Romanian Carpathians and Apuseni Mountains. *Geology* **22**, 807–810.

Peccerillo, A. & Taylor, S. R., 1976. Rare earth elements in East Carpathian volcanic rocks. *Earth and Planetary Science Letters* **32**, 121–126.

Pécskay, Z., Edelstein, O., Seghedi, I., Szakács, A., Kovács, M., Crihan, M. & Bernad, A., 1995*a*. Recent K–Ar dating of Neogene/Quaternary volcanic rocks in Romania. *Acta Vulcanologica* **7**, 15–28.

Pécskay, Z., Lexa, J., Szakács, A., Balogh, Kad., Seghedi, I., Konecny, V., Kovács, M., Márton, E., Kaliciak, M., Szeky-Fux, V., Poká, T., Gyarmati, P., Edelstein, O., Rosu, E. & Zec, B., 1995*b*. Space and time distribution of Neogene–Quaternary volcanism in the Carpatho-Pannonian region. *Acta Vulcanologica* **7**, 53–61.

Peltz, S., Vasiliu, C., Udrescu, C. & Vasilescu, A., 1973. Geochemistry of volcanic rocks from the Călimani, Gurghiu and Harghita Mountains (major and trace elements). *Annarul Institutului Geologic* **xlii**, 339–393.

Peltz, S., Vajdea, E., Balogh, K. & Pécskay, Z., 1985. Contributions to the chronological study of the volcanic processes in the Călimani, Harghita and Persani Mountains. *Dari de Seama Institutul de Geologie si Geofizica* **72**, 323.

Peltz, S., Seghedi, I., Grabari, G. & Popescu, G., 1987. Strontium isotope composition of the volcanic rocks from the Călimani, Harghita and Persani Mountains. *Dari de Seama Institutul de Geologie si Geofizica* **72–73–1**, 309–321.

Pe-Piper, G., 1994. Lead isotopic compositions of Neogene volcanic rocks from the Aegean extensional area. *Chemical Geology* **118**, 27–41.

Rădulescu, D. & Săndulescu, M., 1973. The plate-tectonics concept and the geological structure of the Carpathians. *Tectonophysics* **16**, 155–161.

Roure, F., Roca, E. & Sassi, W., 1993. The Neogene evolution of the outer Carpathian flysch units (Poland, Ukraine and Romania): kinematics of a foreland/fold-and-thrust belt system. *Sedimentary Geology* **86**, 177–201.

Royden, L. H., 1988. Late Cenozoic tectonics of the Pannonian Basin system. In: Royden, L. H. & Horváth, F. (eds) *The Pannonian Basin. American Association of Petroleum Geologists Memoir* **45**, 27–48.

Royden, L. H. & Báldi, T., 1988. Early Cenozoic tectonics and palaeogeography of the Pannonian and surrounding regions. In: Royden, L. H. & Horváth, F. (eds) *The Pannonian Basin. American Association of Petroleum Geologists Memoir* **45**, 1–16.

Royden, L. H. & Burchfiel, B. C., 1989. Are systematic variations in thrust-belt style related to plate boundary processes? *Tectonics* **8**, 51–61.

Salters, V. J. M., Hart, S. R. & Panto, Gy., 1988. Origin of late Cenozoic volcanic rocks of the Carpathian arc, Hungary. In: Royden, L. H. & Horváth, F. (eds) *The Pannonian Basin. American Association of Petroleum Geologists Memoir* **45**, 279–292.

Săndulescu, M., 1988. Cenozoic tectonic history of the Carpathians. In: Royden, L.H. & Horváth, F. (eds) *The Pannonian Basin. American Association of Petroleum Geologists Memoir* **45**, 17–25.

Saunders, A. D., Norry, M. J. & Tarney, J., 1988. Origin of MORB and chemically depleted mantle reservoirs: trace element constraints. *Journal of Petrology, Special Lithosphere Issue*, 415–445.

Seghedi, I., Grabari, G., Ianc, R., Tanasescu, A. & Vajdea, E., 1986. Rb, Sr, Zr, Th, U, K distribution in the Neogene volcanics of the South Harghita Mountains. *Dari de Seama Institutul de Geologie si Geofizica* **70–71/1**, 453–473.

Seghedi, I., Szakács, A. & Mason, P. R. D., 1995. Petrogenesis and magmatic evolution in the East Carpathian Neogene volcanic arc (Romanian). *Acta Vulcanolgica* **7**, 135–143.

Seghedi, I., Szakács, A., Udrescu, C., Stoian, M. & Grabari, G., 1987. Trace elements geochemistry of the Southern Harghita volcanics (East Carpathians): calc-alkaline and shoshonitic associations. *Dari de Seama Institutul de Geologie si Geofizica* **72–73/1**, 381–397.

Socolescu, M., Popovici, D., Visarion, M. & Rosca, V., 1964. Structure of the Earth's crust in Romania as based on gravimetric data. *Revue Roumaine de Géologie, Géophysique et Géographie, Série de Géophysique* **8**, 3.

Stănică, D., Stănică, M. & Pinna, E., 1990. Magnetotelluric soundings in the East Carpathians–Harghita area. *Revue Roumaine Géophysique* **30**, 25–35.

Stern, C. R., 1991. Role of subduction erosion in the generation of Andean magmas. *Geology* **19**, 78–81.

Sun, S. S. & McDonough, W. F., 1989. Chemical and isotopic systematics of oceanic basalts: implications for mantle composition and processes. In: Saunders, A. D. & Norry, M. J. (eds) *Magmatism in the Ocean Basins. Geological Society of London Special Publication* **42**, 313–345.

Szabó, Cs., Harangi, Sz. & Csontos, L., 1992. Review of Neogene and Quaternary volcanism of the Carpathian–Pannonian region. *Tectonophysics* **208**, 243–256.

Szakács, A., Seghedi, I. & Pécskay, Z., 1993. Peculiarities of South Harghita Mts as the terminal segment of the Carpathian Neogene to Quaternary volcanic chain. *Revue Roumaine Géologie* **37**, 21–36.

Taylor, H. P. & Sheppard, S. H. F., 1986. Igneous rocks: I. Processes of isotopic fractionation and isotope systematics. In: Valley, J. W., Taylor, H. P., Jr, & O'Neil, J. R. (eds) *Stable Isotopes in High Temperature Geological Processes. Mineralogical Society of America, Reviews in Mineralogy* **16**, 227–271.

Thirlwall, M. F., 1982. Systematic variation in chemistry and Nd–Sr isotopes across a Caledonian calc-alkaline volcanic arc: implications for source materials. *Earth and Planetary Science Letters* **58**, 27–50.

Thirlwall, M. F., 1983. Isotope geochemistry and origin of calc-alkaline lavas from a Caledonian continental margin volcanic arc. *Journal of Volcanology and Geothermal Research* **18**, 589–631.

Thirlwall, M. F., 1991. Long term reproducibility of multicollector Sr and Nd isotope ratio analyses. *Chemical Geology, Isotope Geosciences Section* **94**, 85–104.

Tomek, C. & Hall, J., 1993. Subducted continental margin imaged in the Carpathians of Czechoslovakia. *Geology* **21**, 535–538.

Vaselli, O., Downes, H., Thirlwall, M., Dobosi, G., Coradossi, N., Seghedi, I., Szakács, A. & Vannucci, R., 1995. Ultramafic xenoliths in Plio-Pleistocene alkali basalts from the Eastern Transylvanian Basin: depleted mantle enriched by vein metasomatism. *Journal of Petrology* **36**, 23–53.

Vroon, P. Z., van Bergen, M. J., White, W. M. & Varekamp, J. C., 1993. Sr–Nd–Pb isotope systematics of the Banda Arc, Indonesia: combined subduction and assimilation of continental material. *Journal of Geophysical Research* **98**(B12), 22349–22366.

Watson, E. B., 1982. Basalt contamination by continental crust: some experiments and models. *Contributions to Mineralogy and Petrology* **80**, 73–87.

White, W. M. & Dupré, B., 1986. Sediment subduction and magma genesis in the Lesser Antilles: isotopic and trace element constraints. *Journal of Geophysical Research* **91**(B6), 5927–5941.

Whitford, D. J., White, W. M. & Jezek, P. A., 1981. Neodymium isotopic composition of Quaternary arc lavas from Indonesia. *Geochimica et Cosmochimica Acta* **45**, 989–995.

Wilson, M. & Downes, H., 1991. Tertiary–Quaternary extension related alkaline magmatism in Western and Central Europe. *Journal of Petrology* **32**, 811–849.

Wörner, G., Harmon, R. S. & Moorbath, S., 1992. Andean Cenozoic volcanic centres reflect basement isotopic domains. *Geology* **20**, 1103–1106.

RECEIVED FEBRUARY 1, 1995
REVISED TYPESCRIPT ACCEPTED MARCH 19, 1996